INNATE IMMUNITY OF THE NEMATODE WORM *CAENORHABDITIS ELEGANS,* ITS INTERACTION WITH THE BACTERIAL PATHOGEN *BURKHOLDERIA THAILANDENSIS*, AND THE NATURE OF DEFENSIN-LIKE PEPTIDES

By

Benjamin R. Patterson

A Thesis

Presented to

The Faculty of Humboldt State University

In Partial Fulfillment

Of the Requirements for the Degree

Master of Arts

Biology

May 2008

ABSTRACT

INNATE IMMUNITY OF THE NEMATODE WORM *CAENORHABDITIS ELEGANS,* ITS INTERACTION WITH THE BACTERIAL PATHOGEN *BURKHOLDERIA THAILANDENSIS*, AND THE NATURE OF DEFENSIN-LIKE PEPTIDES

Benjamin R. Patterson

The science of immunology, for much of its history, has focused on the ability to induce the biological acquisition of specific immunity or on the ability to produce specific immune agents. Examples are, respectively, vaccinations that enable vertebrate animals to become completely immune to a specific microbe, and production of specific antiserums and antibodies that can be used to directly treat illness, or to study cellular biology. In modern times a new appreciation for non-adaptive immune measures, a.k.a. innate immunity, has begun to emerge. It has become increasingly clear that non-adaptive measures carry out a massive portion of the work done in keeping multicellular organisms immune. This work includes the quintessential functions of self/non-self recognition and initiation of adaptive responses.

In the last ten years the nematode worm *Caenorhabditis elegans* has begun to be used as an effective model organism for the study of innate immunity. It has been shown that this worm engages in recognition of pathogens via pathogen associated molecular patterns (PAMPs), that it uses conserved cellular signaling pathways during its immune response, that it constitutively produces conserved microbicidal measures, and that it responds to infections by inducing expression of conserved microbicidal effectors.

In the current study I have exposed *C. elegans* to the bacterial pathogen *Burkholderia thailandensis,* which is a nearly identical pathogen to the causative agent of the human disease Melioidosis (*Burkholderia pseudomallei*). I did this in an effort to shed some light on the nature of this infection. Specifically, I exposed *C. elegans* worms to living bacteria and to bacterial exometabolites. I then measured the expression of genes known to be involved in the worm's immune function. In addition, I compared the CSαβ-type (defensin-like) peptides of this worm to putative protein sequences from the human genome and discovered a high degree of identity in some examples. My results show that the worm is responding immunologically to *B. thailandensis* and that this microbe's exotoxic effects are having direct impact on the worm's expression of at least one CSαβ-type peptide. In addition, my results suggest that there may be a class of CSαβ-like peptide that has been previously uncharacterized.

ACKNOWLEDGEMENTS

I have to give a special thanks to my thesis advisor Dr. Jacob Varkey for providing me with the inspiration for these procedures and for providing the means by which to carry them out. I must also give a prominent thanks to the Howard Hughes Medical Institute for my funding. I thank my committee members for their support during the process of completing this thesis. Dr. Mark Wilson, from my committee, deserves a special thanks for inspiring me to use bioinformatics tools for the characterization of genetic and proteomic properties. I thank Dr. Jonathan Ewbank of The Centre d'Immunologie de Marseille-Luminy for his help with my understanding of the *C. elegans* immune system. Anthony Backer of the Biological Sciences stock room also deserves a special thanks for setting up and calibrating the real-time PCR machine. I would like to thank Terry Jones of the bacteriology stock room for his help with bacterial strains. I must also acknowledge my good friend Wolfgang Meyers for his help getting a significant quantity of source code working on local computers. I want to thank all of the undergraduate students who worked with me on this project and I want to thank the Biological Sciences Department at Humboldt State University for their years of excellent service to me during my education.

TABLE OF CONTENTS

TABLE OF CONTENTS (continued)

TABLE OF CONTENTS (continued)

LIST OF TABLES

LIST OF TABLES (continued)

LIST OF FIGURES

LIST OF FIGURES (continued)

INTRODUCTION

Immunobiology is one of the most important avenues of scientific inquiry in modern times, and most people are well aware that animals must be capable of protecting themselves against microbes. Concepts such as germs, immunization and sanitation are commonplace in society, and current public health crises like the spread of the Human Immune Deficiency Virus (perhaps the epitome of a disease agent that targets the human immune system) demonstrates the importance of the immune system to the general public on a regular basis. The amount of time and money that has been funneled into deciphering the intricacies of immunobiology is truly gigantic, and millions of people have lived longer and healthier lives as a result of it.

A Short History of Immunobiology and the Importance of Innate Systems

The beginning of the science of immunology is usually placed about 220 years ago when Edward Jenner demonstrated that inoculating human beings with cowpox could effectively protect those people from future infections with smallpox (Jenner 1801, Mazumdar 2003). Historically speaking, however, the first smallpox vaccinations were being carried out in China possibly starting in the 5th century A.D., more than 1200 years before Dr. Jenner's experiments. The Royal Society in England became aware of the Chinese method in 1700, nearly 100 years prior to Jenner's experiments. Similar methods existed in India and Turkey at the time, and the Turkish method of smallpox immunization became popular among some of the English aristocracy starting around

1750. During this period, a researcher for the English Royal Society empirically concluded that whereas virtually everyone caught smallpox and the death rate was about 1 in 7, those treated with the Turkish method appeared to be completely immune and the death rate from the procedure was 1 in 50. In addition to this, those who survived smallpox infections were often left with chronic health problems which shortened their lives. Immunized individuals did not have this problem. During the latter half of the 18th century in England, it was also observed that individuals who caught cowpox (a related but much less severe disease than smallpox) seemed to be immune to smallpox. It was in this context that Dr. Jenner did his experiments, and the broadly unpopular mandatory vaccinations that resulted (imposed by the English government on its people) significantly reduced the spread of the disease in England. Not only was the rate of smallpox infection greatly reduced, but many of the associated "survivor diseases" were largely eradicated (Mazumdar 2003).

From its earliest inception, the study of immunology has been, largely, the study of the ability of organisms to develop specific responses to specific disease agents. This theme has dominated much of immunology's practical applications and its laboratory research projects for much of its history. This is interesting because the ability to acquire specific immunities, which exists only in vertebrates, is actually the smaller (but still *very* important) part of the human immune system. The larger and far more ancient part of human immunity, the innate immune system, does not acquire immunity and uses some mechanisms that appear to be common (in at least one form or another) to all multicellular life (Mazumdar 2003, Beutler 2004, Medzhitov 2003).

Inquiries into immune mechanisms that would now be considered to be innate have been occurring since as early as the beginning of the 20th century, but they have tended to be overshadowed by the experimental and social efficacy of the highly specific acquired immune mechanisms. As early as the first decade of the 20th century, prominent laboratories were focusing significant effort on the study of the cellular basis of immunity, and at least one Nobel Prize was awarded to individuals who observed important innate mechanisms. At the same time, however, the labs that were studying adaptive mechanisms were producing powerful serums that were effective medicines for major diseases such as typhoid and diphtheria, and sold for significant profit. Adaptive mechanisms are also responsible for the efficacy of the vaccines that are commonplace in the modern era, and the Human Immune Deficiency Virus (HIV), which has commanded a massive portion of the resources devoted to immunology in modern times, specifically targets those adaptive mechanisms (Mazumdar 2003, Beutler 2004, Medzhitov 2003). For reasons such as these, when most people think of immunity, they think of adaptive immunity: “Oh, I already had that one. I won’t get it again.”

This being said, available evidence suggests that the adaptive immune system does a small percent of the actual work of protecting us from infection (Beutler B. 2004, Medzhitov R. 2003, Janeway et al. 2005, Akira et al. 2006) and its ability to acquire specific immunities and memory of past infections are ultimately the result of a single, highly conserved set of genes that originated early in vertebrate evolution, the Recombination Activating Genes (RAG). These are the genes that are responsible for the structural rearranging of B- and T-cell receptors in lymphocyte progenitors which leads

to millions of permutations of these receptors, and thus, to the ability to acquire specific immunities (Beutler 2004, Medzhitov 2003, Paul 2003, Janeway et al. 2006).

In contrast, the innate immune system does the large majority of the work of keeping us immune, and relies on a large number of diverse genes, some of which originated hundreds of millions of years before the appearance of vertebrates. Innate immune receptors are hard wired in the genome, and innate responses to infection are often not of common evolutionary origin. The innate immune system does not acquire specific immunities, does not have memory of past invaders and is, fundamentally, the sentinel that identifies the presence of non-self in our bodies. In a very real sense, the adaptive immune system is simply the branch of the innate immune system that has evolved the ability to develop receptors specific to a given antigen and to remember which receptors have worked the best (Beutler 2004, Medzhitov 2003, Paul 2003, Janeway et al. 2006). In the past 30 years or so a true understanding as to the fundamental importance of the innate immune system in directing the immune response has begun to emerge (Mazumdar 2003).

In general, innate immune systems share at least a couple of common features. First is the ability to distinguish self from non-self. This is accomplished by a combination of two approaches: recognition of non-self molecules and recognition of missing self (though there seem to be some conflicting results on the latter). The first is certainly the more established of the two and is achieved by the host recognizing biochemical components of a given pathogen, termed pathogen associated molecular patterns (PAMPs). These are usually some form of molecule that is essential for the

pathogen's biology but foreign to the host's biology (Medzhitov 2003). Evolution has selected for this type of marker for two main reasons: 1) biomolecules that are essential to the pathogen are not easily lost by that pathogen through evolution, and 2) biomolecules that are alien to the host are effective markers for the presence of non-self. Examples of PAMPs include lipopolysaccharide (LPS), lipoteichoic acids, peptidoglycan, and beta-glucans to name a few of the multitude. An example of a self marker that can be absent in missing self-recognition is the major histocompatibility complex (MHC) molecules of mammals. Our immune systems will respond to both types of signals by trying to kill the cells that either have the PAMPs, or do not have the self markers on their surfaces (Medzhitov 2003).

The host receptors that recognize PAMPs are, in turn, termed pattern recognition receptors (PRRs) and tend to be of diverse evolutionary origin. They are referred to as PRRs because in some prominent examples it is not the uniqueness of the molecule on the surface of the pathogen that is responsible for non-self recognition but instead the pattern of their arrangements. For example, both mammalian and bacterial cells have glycosylated peptide structures on their surfaces, but the surfaces of mammalian cells have a fluid nature, where any particular geometric arrangement of surface markers is somewhat transient, and bacteria have dense solid repeating patterns (for example, the lattice structure of peptidoglycan) where the sugar substituents are repeating and not transient. Mannose-binding lectin (discussed below) in our own immune system recognizes specifically this dense pattern, even though its individual binding domains

have no more affinity for bacterial sugars than they do for mammalian sugars (Medzhitov 2003, Turner and Hamvas 2000).

The second feature of innate immune systems is that they respond when they encounter a pathogen. These responses are diverse but all attempt to impart on the host, in one way or another, resistance to the given invader. These responses include secretion of antimicrobial proteins and peptides, increased production and "bursts" of reactive chemical species, compartmentalization of infected areas, changes in normal homeostasis of the host, signaling between various cells of the host, and, in the case of vertebrates, induction of events that lead to the activation of adaptive immunity (Mazumdar 2003, Beutler 2004, Medzhitov 2003, Janeway et al. 2005, Akira et al. 2006, Paul 2003, Turner and Hamvas 2000).

An Example of the Human Innate Immune Response

The ultimate goal in much of the study of immunology is to learn how to more effectively treat human disease. Below is a theoretical example of the progression of the human innate immune response intended to demonstrate the sheer magnitude of work done by these systems, and, therefore, to show the importance of studying these systems. This is only a brief overview, leaving many of the details out. Bear in mind that much of what is known about these human systems was learned by studying model systems. Our bodies use an integrated innate system of barriers, constitutive defenses, pattern recognition, signaling, altered cellular behavior, induction of microbicidal measures, compartmentalization and, finally, system-wide responses to effect our immunity.

This example includes the skin as an epithelial barrier that must be crossed by an invader, but in basic principal, multiple epithelial surfaces are engaged in similar types of activity to defend themselves against pathogens. These activities include continuous renewal of surface material, harboring of commensal microbes, formation of a contiguous barrier between outer/luminal spaces and the internal body tissues, harboring of professional immune cells, and constitutive expression of antimicrobial substances (Tlaskalová-Hogenová et al. 2002).

The first challenge a potential invader will encounter is, in fact, adherence to the surface of our skin. Our skin is constantly renewing itself, flaking off old cells and replacing them with underlying new cells. A potential pathogen may also face stiff competition for a point of adherence from commensals (Tlaskalová-Hogenová et al. 2002). If an invader is able to establish adherence in spite of these challenges, it will next face constitutively expressed antimicrobial effectors including but not limited to lysozyme (though this is expressed only cytoplasmically in the dermal and epidermal cells), dermcidin, cathelicidin LL-37, RNase 7, and psoriasin (Schröder and Harder 2006).

If the invader can survive these and it can breach the outer cells (the stratum corneum), it will reach the living cells of the stratum germinativum, composed mostly of karatinocytes (Gröne 2002). These cells contain numerous PRRs, including several in the Toll-like receptor (TLR) family (Köllisch et al. 2005). The invader will encounter these cells, and these cells will, in turn, recognize the presence of non-self via their PRRs. In turn, this will induce signal transduction through highly conserved intracellular signaling

pathways (such as Toll-like receptor pathways) that result in the expression of numerous inflammatory cytokines, chemokines and a myriad of inducible microbicidal proteins on top of those constitutively expressed in the epidermis (Schröder and Harder 2006, Gröne 2002, Köllisch et al. 2005). Mammalian TLRs and cytokines/chemokines are reviewed in Akira at al. 2006, and in Borish and Steinke 2003, respectively.

Some of the cytokines produced will, in turn, activate cytokine receptors on adjacent cells, which will subsequently proliferate an inflammatory response in these cells. The inflammation process will biologically establish a point of infection in the skin, and the chemokines released by this positive feedback process will diffuse away from this point as a beacon to other cells as to the infection's location.

Specific cytokines, for example IL-1, mediated through cell surface receptor binding will cause the swelling of local blood vessels (capillaries, arterioles and venules), the loosening of vaso-endothelial tight junctions and the expression of ICAM-1, VCAM-1 and E-selectin on the luminal surface of vaso-endothelial cells. These surface markers, along with the chemokines originating from the point of infection, will cause the extravasation of leukocytes, including neutrophils, macrophages, B-cells, dendritic cells and natural killer cells (Beutler 2004, Medzhitov 2003, Borish and Steinke 2003, Santana and Esquivel-Guadarrama 2006). In addition, immune cells resident in the skin including dendritic cells and lymphocytes will be drawn to the point of infection by chemokines (Gröne 2002, Santana and Esquivel-Guadarrama 2006).

All of these immune cells are capable of being excited by inflammatory cytokines and will engage in a bombardment of the invader by antimicrobial measures. These

include secretion of antimicrobial peptides and proteins, degranulation, phagocytosis/ endocytosis, proteolysis, reactive oxygen bursts, cytotoxic responses and more (Beutler 2004, Medzhitov 2003). In addition to these responses, B-cells, dendritic cells and macrophages (the main types of antigen presenting cells [APCs]) can digest phagocytosed invaders, process the antigens and present them on MHC class molecules (Santana and Esquivel-Guadarrama 2006). Another very important response of all of these cells is the further production of cytokines and chemokines via activation of cytokine receptors and PRRs, allowing for further ramping up of the inflammatory response in the case of a pernicious invader (Medzhitov 2003, Gröne 2002, Borish and Steinke 2003, Santana and Esquivel-Guadarrama 2006).

If the invader is able to survive this onslaught, it may force or digest its way through the surrounding tissues. When blood enters the infection from broken blood vessels, or the invader begins forcing its way into the blood serum, the serum PRR, mannose-binding lectin, will adhere to repeating sugar units on the invader's surface and initiate what is known as the MBL-initiated complement cascade (Janeway et al. 2005). This will lead to opsonization, which will increase phagocytic activity of immune cells, and the formation of the membrane attack complex, which will directly kill the invader. Intermediates of the complement cascade also act as receptor-mediated inflammatory signals (which again can ramp up the inflammatory response) and as initiators of the coagulation cascades in the blood, which will seal off the blood vessel and prevent the invader from using the bloodstream as a dispersal method (Peterson et al. 2001, Sjöholm et al. 2006, Sims and Wiedmer 1995).

As the invader persists and multiplies, the build up of inflammatory cytokines (for example, IL-1 and IFN-α) can begin reaching the central nervous system and this, in turn, can lead to changes in homeostasis. Two changes that are known to occur are fever and increased production of MBL into the blood serum (Janeway et al. 2005). In addition, if the invasion persists long enough, then many APCs (most importantly dendritic cells) will have molecular components of phagocytosed invaders presented on MHC-I or MHC-II class molecules, and these cells will, subsequently, follow chemokines (for example, CCL19 and various forms of CCL21) toward lymphatic vessels. Once reaching the lymph nodes, they will initiate type-1 and/or type-2 adaptive immune responses (Santana and Esquivel-Guadarrama 2006).

This truncated overview of a hypothetical immune response hopefully makes clear the enormous job done by our innate systems. Every aspect of the immune process described above occurs in real world examples with neither unique specificity nor memory developing. It is all the product of receptors and associated organismal responses that are germline encoded and ancient in evolution. Without these innate responses adaptive responses would not exist.

The Importance of Models in Immunobiology

Drosophila melanogaster as model organism needs no introduction. In the mid 1980s, the *Toll* gene was identified through screens for maternal effect genes in the fly. It was shown that *Toll* is required for proper dorso-ventral development in embryos. (Gerttula et al. 1988). In the nineties it was shown that the Toll transmembrane receptor

was involved in the resistance of adult *Drosophila* to fungal pathogens (Lemaitre et al. 1996) and that multiple homologs exist in human beings (Rock et al 1998). Through further study, including much work done in mouse and rat models, 13 Toll homologs (the Toll-like receptors or TLRs) have been identified, 10 of which are expressed in human beings. These receptors are centrally important in the initial recognition of non-self in a massive diversity of multicellular life, including plants. In human beings they are indispensable in our immunity and many loss of function mutants result in severe immune deficiency. TLRs represent one of the long-elusive mechanisms of self/non-self determination, and their existence would likely still be unknown were it not for their identification in screens of *Drosophila* maternal effect genes (Beutler B. 2004, Medzhitov 2003, Akira et al 2006, Lemaitre et al 1996, Rock et al. 1998).

TLRs in general have some conserved features. They are all class 1 integral membrane proteins that have an extracellular (or vesicular luminal) ligand binding domain and a cytosolic signaling domain. The outer domain contains varying numbers of leucine-rich repeat motifs and the cytosolic domain is homologous to the interleukin-1 receptor. In mammalian systems, 13 TLRs are known for recognizing at least 25 PAMPs. The mechanism by which individual TLRs can recognize multiple, unrelated PAMPs is still somewhat elusive. However, it is due at least in part to the differential complexing of TLRs during ligand binding, and to the specific location of the TLR on or within the cell. The cytosolic Toll/interleukin-1 receptor (TIR) domains are active in signaling as dimers (and possibly higher order structures), and can effect different combinations of downstream signaling cascades based on which TLRs are complexed with which ligand

(Akira et al. 2006, Beutler 2004, Medzhitov 2003). The conserved signaling pathways are discussed in these references. However, I will not get into them here. Suffice to say that there is a great deal of conservation within the signaling cascades of TLRs. There is also significant divergence between distantly related phyla.

Caenorhabditis elegans as a Model for Innate Immunity

Since the late 1990s, *Caenorhabditis elegans* has emerged as a model for the study of conserved mechanisms of innate immunity due to its many longstanding advantages as a model organism, its concerted immune effort against microbes and its susceptibility to a number of important human pathogens. The *C. elegans* immune system has been extensively reviewed and shares several features in common with our own. These include physical barriers with constitutive antimicrobial measures, pathogen recognition, induction of signaling pathways, altered organismal and cellular behavior, and secretion of inducible antimicrobial proteins (Gravato-Nobre and Hodgkin 2005, Kim. and Ausubel 2005, Mylonakis and Aballay 2005, Sifri et al. 2005, Millet and Ewbank 2004, Schulenburg et al. 2004, García-Lara et al. 2005, DeVeale et al. 2004, Ewbank 2002, Kurz and Ewbank 2003, Alegado et al. 2003, Pradel and Ewbank 2004).

Modes of infection

Pathogens that infect *C. elegans* can be thought of as having 5 possible modes of pathogenesis: 1) gut colonization, in which pathogenic microbes form a persistent population in the gut of the worm that leads, often, to severe distension and possibly death; 2) persistent infection, which differs from gut colonization only in that when the

worm is moved into non-pathogenic bacteria the infection persists, suggesting possible bacterial adherence to gut epithelium; 3) invasion, in which the pathogen adheres to the cuticle and penetrates the worms body; 4) biofilm formation, in which the pathogen adheres to the cuticle and forms a biofilm over its surface, notably the mouth; and 5) toxin mediated killing, in which the bacterium kills the worm with either an endotoxin or exotoxin (Gravato-Nobre and Hodgkin 2005, Kim and Ausubel 2005, Sifri et al. 2005).

The main physical barrier surrounding the worm is its cuticle and five notable pathogens (*Drechmeria coniospora, Microbacterium nematophilum, Yersinia pestis, Yersinia pseudotuberculosis* and *Duddingtonia flagrans*) are able to bind to this surface and gain entry into the worm through the progression of subsequent events. Mutations in *srf* genes, which alter the exterior surface of the worm, result in worms that vary in their resistance to four of these pathogens: the two *Yersinia* species mentioned above, *D. coniospora* and *D. flagrans*. Pathogens that can adhere to the outer surface of the worm, however, are quite the minority in known examples. The two most common modes of pathogenesis are intestinal colonization and toxin-mediated killing (Gravato-Nobre and Hodgkin 2005, Kim and Ausubel 2005, Mylonakis and Aballay 2005).

In the case of gut colonization, the pathogen must get past what appears to be constitutive antimicrobial secretions in the pharynx and must also get past the pharyngeal grinder in order to reach the intestine (Gravato-Nobre and Hodgkin 2005, Mylonakis and Aballay 2005). The proteins *ABF-1* and *ABF-2* (antibacterial factors 1 and 2) have been shown to be expressed constitutively in the pharyngeal lumen using GFP reporters, and *ABF-2* has been shown to have potent antimicrobial activity against bacteria and yeast.

However, to my knowledge no direct correlation has been made between *C. elegans* aberrant in *ABF* expression and hypersusceptibility to infection (Gravato-Nobre and Hodgkin 2005, Kato et al 2002). Mutations that affect grinder function, on the other hand, result in worms that are far more susceptible to specific infections. For example, *phm-2* mutants that have resultant defective grinder function are hypersusceptible to infection by the pathogens *Salmonella enterica* and *Pseudomonas aeruginosa*, bacteria that colonize the gut (Gravato-Nobre and Hodgkin 2005).

In the case of toxins, some are far more potent than others, and some have been fairly well characterized while others have not. For example, it has been well demonstrated that the toxin from *Bacillus thuringiensis* Cry5B is a pore forming toxin. And it has been shown that one of the responses of the worm is to up regulate *ttm-1* and *ttm-2*, possibly helping to reduce the damage caused by ionic imbalance due to pore formation. Another reaction of the worm to these pore-forming toxins is to activate a JNK-like MAP kinase cascade, which is known to be involved in the worm's response to heavy metal stress (Gravato-Nobre and Hodgkin 2005). Another example of a toxin is the apparent neurotoxin secreted by several *Burkholderia* species. In contrast to the pore forming toxin discussed above, this toxin is virtually uncharacterized. It is clear that it causes paralysis of the worms in a relatively short amount of time, generally beginning to take effect by 24 hours following exposure. It also seems that these bacteria employ some mechanism of active pathogenesis, as evidenced by the slower rate of killing when exposed to toxin alone (Gan et al. 2002).

Pathogen recognition

To date there are no described PRRs in *C. elegans*, though, in light of its pointed immune response to pathogens (many of them pathogens to the worm in its natural habitat), these receptors must exist. Of particular interest in the search for these receptors is the 125 C-type lectin sequences present in the *C. elegans* genome. Of these, 10 have membrane-association domains (Schulenburg et al. 2004). In addition, three lectins were shown to be upregulated in their expression in response to *Serratia marcescens* infection, suggesting that these particular examples are, perhaps, PRRs involved in some sort of immune positive feedback system (Mallo et al. 2002). It is also of particular interest that the *C. elegans* genome contains all the necessary components for a complement cascade, which is an innate immune mechanism that is highly conserved across a broad diversity of multicellular life (Schulenburg et al. 2004).

Another possibility for potential PRRs are chemoreceptor genes that are expressed in the nervous system. There are more than 1000 sequences in the worm's genome that resemble G-protein-coupled transmembrane receptors. More than 500 of these have been suggested to be functional in its nervous system chemoreception. Some could be involved in neural control of the immune response (Schulenburg et al. 2004). There is some evidence to suggest that such a process may, in fact, occur in this worm. The worm's only Toll homolog, *tol-1,* has been observed to be involved in its avoidance of pathogenic bacteria that have been spotted on a plate. Specifically, *tol-1* mutants fail to avoid *S. marcescens* after several hours of exposure when this bacterium is spotted on a plate along with the worms (Gravato-Nobre and Hodgkin 2005). In light of Toll's highly

conserved function as a PRR across other lineages, it is possible that in *C. elegans* this homolog is functioning as a PAMP-recognizing neuroreceptor.

Signaling

There are six signaling pathways involved in *C. elegans* immunity. These are the p38 MAP kinase cascade, the JNK cascade, the ERK cascade, a TGF-β-like pathway, the programmed cell death pathway and the DAF-2 (insulin-receptor like) pathway. These are conserved pathways and several are well established in stress and immune responses in other organisms. For example, the specific TGF-β pathway involved in *C. elegans* immunity (DBL-1) is known for its function in both *Drosophila* and mammalian immunity. Another example is the ERK cascade, which has a well established immune function in plants (Gravato-Nobre and Hodgkin 2005, Millet Ewbank 2004).

TGF-β-like pathway. This pathway is known for its function in controlling morphology in *C. elegans* male tail development (among other things) and it is variably called the small/male tail abnormal (Sma/Mab) or the Decapentaplegic/bone morphogenic protein-like (DBL-1) pathway. Of interest, lysozyme-8 (a *C. elegans* homolog of a known immune effector protein that targets peptidoglycan) is a target of this pathway. Of additional interest, three of this pathway's known targets are C-type lectins, again suggesting that this pathway may be involved in a possible mechanism of immune positive feedback, though there is no direct evidence of these gene, specifically, being upregulated by the TGF-β-like pathway in response to infection. Another factor thought to be part of this signaling cascade (based on homology with mammals) is the

transcription factor *mef-2*. In mammals this transcription factor is thought to be involved in crosstalk between the TGF-β pathway and the mammalian homolog of the p38 MAPK pathway. Mutations in *mef-2* lead to worms that are hypersusceptible to infection (Millet and Ewbank 2004).

p38 MAP kinase cascade. This cascade is probably one of the oldest signaling pathways involved in immunity, as evidenced by its conservation in all metazoan lineages that have been examined for its presence (Millet Ewbank 2004). In *C. elegans* it is known to be important in mediating the response to heavy metal stress and bacterial toxins. Specifically, this cascade is responsible for the upregulation of *ttm-1* and *ttm-2* in response to the *B. thuringiensis* pore-forming toxin, as previously mentioned. An interesting example of a likely immune specific function of this pathway (as opposed to a general stress response) involves the only *C. elegans* protein aside from TOL-1 that shows any Toll homology, TIR-1. This protein is critical for inducing expression of the potent antifungal NLP-31, and it signals through the p38 MAPK cascade. Of evolutionary interest, the TIR signaling in *C. elegans* is unique with respect to other known examples, and this has led some to propose, based on the nature of the homologies of various TIR signaling components between species, that TIR signaling in *C. elegans* is the most ancient known example (Kim and Ausubel 2005).

JNK pathway. This pathway is known to be involved in heavy metal response and is, apparently, one of the possible downstream signaling pathways activated by the p38 MAPK pathway. Its function in the worm's immune system may be limited to a general response to the toxins employed by some pathogens. For example, this pathway is

responsible for protecting the worm against the pore-forming toxin of *Bacillus thuringiensis,* already mentioned. This protection occurs in a p38-dependant way. However, abrogation in the JNK pathway does not lead to general hypersusceptibility of the worm to pathogens, suggesting that JNK activation is only one of the possible downstream signaling fates of the p38 MAPK cascade (Gravato-Nobre and Hodgkin 2005).

ERK MAPK pathway. This pathway is, perhaps, one of the most important examples of a pathway that shows an immune specific response to an ecologically relevant *C. elegans* pathogen. As mentioned above, this pathway has well established immune function in plants. In the worm, this pathway is involved in numerous biological functions, including male spicule development, transmission of sensory signals and regulation of fluid balance. This pathway's immune specific function arises in *Microbacterium nematophilum* infection. These bacteria are known to attack the worm in its natural habitat and they do so by adhering to the cells surrounding the anus. In response these cells swell profusely in an ERK MAPK dependent action. Abrogation of the swelling by destruction of the ERK pathway results in a far shorter life expectancy for the worms under challenge by these bacteria. Most of the biological activities for the ERK pathway occur after the pathway is activated by a Ras protein, LET-60. However, this tail swelling apparently occurs in a LET-60 independent fashion (Gravato-Nobre and Hodgkin 2005, Kim and Ausubel 2005). This example represents a scenario in which a central pathway in the worm's biology has a permutation in its function that is specifically an immune response to a coevolving pathogen. This is a significant

observation in itself because it is, in fact, the case that many immune functions in all organisms appear to be processes that have been co-opted from other essential host biological functions in order to protect that host from a specific type of pathogen, a very good example being *Drosophila's* Toll.

Programmed cell death pathway. This pathway is interesting in that it is not clear how it protects the worm against infection. *S. enterica,* when it colonizes the gut, induces germline programmed cell death (PCD), and this has been clearly demonstrated to be important for the worm's survival given challenge by these bacteria. However, the germline cells are not in contact with the invader (Gravato-Nobre and Hodgkin 2005, Mylonakis and Aballay 2005). Several suggestions have been made to explain how this germline PCD may help the worm with protecting itself against infection; all are hypothetical at this time. One suggestion is that the PCD pathway functions not only in programmed cell death, and that once induced it can carry out multiple functions, one of which is cellular activities that protect the gut from *S. enterica.* In this example, the germline PCD would be a symptom of the pathway becoming active, not the cause of the protection observed by it (Mylonakis and Aballay 2005). Of additional interest in this pathway is the observation that *S. enterica* with altered LPS fails to induce PCD, suggesting the existence of a PRR that can specifically recognize LPS in *C. elegans* (Sifri et al. 2005).

Insulin-like (DAF-2) pathway. This pathway was originally identified as being involved in formation of the dauer stage during *C. elegans* maturation. Subsequently, this pathway has been shown to be important for many biological activities, including

longevity, thermotolerance, UV resistance, motility and more. In the context of immunity, abrogation of *daf-2* leads to worms that are more resistant to bacterial infection. In support of an immune specific response, the pathway is known to be an upstream regulator of several known and putative antimicrobial effector proteins, including LYS-7, LYS-8, thaumatins (proteins known for their immune contribution to plants), and several C-type lectins.

Current Study

The above discussion of *C. elegans* immunity should demonstrate that a significant amount has been discovered with respect to this worm's immunity to pathogens. It should be emphasized, however, that most of the intricacies are probably as-of-yet undescribed. Significant questions remain, for example, what are the PRRs of *C. elegans*? Another important question is what are the subtle differences in ligand binding and signal complex formation that result in variable downstream effects from a single signaling cascade? Also, and importantly for my work, the vast majority of pathogens that have been described for this worm have not been extensively studied as per their pathogenesis. Any one of these pathogens may be involved in important, as-of-yet unknown host pathogen interactions.

Genes

In this study I chose to examine some of the aspects of the interaction, on a genetic basis, between *C. elegans* and a relatively little studied pathogen: *Burkholderia thailandensis.* Specifically, I decided to observe the regulation of 6 genes of known and

putative immune function when *C. elegans* is infected by this pathogen. The genes were lysozyme 1 (*lys-1*), lysozyme 7 (*lys-1*), lysozyme 8 (*lys-8*), neuropeptide-like protein 29 (*nlp-29*), antibacterial factor 1 (*abf-1*) and antibacterial factor 2 (*abf-2*). None of these genes have been looked at with respect to their possible role in defense against *B. thailandensis.* The first four are known to be involved with *C. elegans* immunity. The last two are putative in their immune function. All are discussed in greater detail below.

Lysozyme 1 (*lys-1*). Lysozyme is an enzyme that catalyses the hydrolysis of peptidoglycan, and therefore leads to the lysis of bacteria due to loss of cell wall integrity. This gene is one of at least 24 genes in *C. elegans* that show homology to specific amoeboid lysozymes, an observation which in itself is significant because animal species from insects to humans show homology between their lysozyme genes, whereas *C. elegans'* lysozyme genes show homology to what is likely a far more ancient form found in amoeboid protozoa (Mallo et al. 2002, 36). These protozoa apparently use lysozyme synergistically along with other bactericidal compounds to digest bacteria that they phagocytose for food. The idea that multicellular innate immune mechanisms, including our own, may go all the way back to some of the first single-celled eukaryotes is deeply interesting.

In *C. elegans, lys-1* was one of several genes that were verified as being over expressed in *fer-15* mutants (a conditional mutation that results in sterile worms) using microarray and northern blot analysis of mRNA isolated from worms exposed to *Serratia marcescens* (Mallo et al. 2002). In the said study, GFP reporters which included the *lys-1* promoter sequence showed expression in the IL1 and IL2 neurons, the nerve ring and in

what appeared to be vesicles of the gut epithelium. The *fer-15* mutant was used to prevent multiple generations from being present in infections after multiple days, and because this mutant appears to have wild-type resistance to *S. marcescens* (evidenced by near identical disease progression) indicating the likelihood of a normal immune system. I included this gene in my studies as a positive control. I needed to have a known expression pattern that I could use to verify that my procedures would deliver expression results consistent with others in literature.

Lysozyme 7 (*lys-7*). This gene was also shown to be upregulated under exposure to *S. marcescens* (Mallo et al. 2002). I chose to investigate its expression level in this study because it is down stream of the DAF-2 pathway and may be indicative of DAF-2 pathway activation. There is the distinct possibility of extensive crosstalk between the pathways involved in *C. elegans* innate immunity (Ewbank 2006), meaning that induction of this gene may not be conclusive evidence of the DAF-2 pathway becoming activated. However, no gene regulation has been looked at with respect to *B. thailandensis* infection of this worm, and this gene, if changed in expression pattern by *B. thailandensis,* may indicate DAF-2 signaling.

Lysozyme 8 (*lys-8).* Like *lys-1* and *lys-7,* this gene has been shown to be upregulated in the worm's immune response to *S. marcescens*. I chose this one because it's expression is regulated by the DBL-1 pathway (Ewbank 2006). As with *lys-7*, the likelihood of extensive crosstalk between the pathways involved in immunity means that expression of this gene alone may not be definitive evidence of DBL-1 pathway activity.

Its expression in response to *B. thailandensis* would still represent evidence of the DBL-1 pathway's possible involvement.

Neuropeptide-like protein 29 (*nlp-29*). This gene was identified using microarray analysis as one of two genes upregulated in *C. elegans* in response to both *D. coniospora* and *S. marcescens.* There are nine *nlp* genes in the worm and they are so named due to minor sequence similarity to YGGWamide neuropeptides. Using a GFP reporter construct, *NLP-29* was shown to be expressed constitutively, at a low level, in the hypodermis, and to be inducible, increasing many fold in concentration in the hypodermis and in the cells surrounding the vulva, right where *D. coniospora* adheres when it is invading this worm (Couillault et al. 2004).

Chemically synthesized NLP-31 is strongly antifungal and also shows microbicidal activity against Gram negative and Gram positive bacteria. Both NLP-29 and NLP-31 appear to be downstream of TIR-dependent signaling in that RNAi knockout of *tir* expression leads to worms that are significantly handicapped in their ability to produce NLP-29. I chose to look at the expression of this gene due to that fact. As with the above examples, upregulation of *nlp-29* in the face of challenge by *B. thailandensis,* may indicate TIR signaling, but would not, by itself, rule out crosstalk from other pathways.

Antibacterial factors 1 and 2 (*abf-1 & abf-2*). These genes are members of the ASABF-type (*Ascaris suum* antibacterial factor) proteins so named for their role in protecting the parasitic *A. suum* nematode from bacteria. Injection of heat-killed bacteria into the pseudocoelomic cavity caused pointed upregulation of several of these genes in

A. suum (Pillai et al. 2003). The ASABF proteins in both *A. suum* and *C. elegans* also contain a conserved cysteine motif found in insect defensins. The *C. elegans* homolog, ABF-2, proved to be potently antimicrobial against Gram negative bacteria, with Gram positive bacteria and fungi varying in their sensitivity to it from very sensitive to essentially immune. At the moment, evidence suggests that the ASABF homologs in *C. elegans* may represent part of the worm's immune arsenal (Kato et al. 2002).

C. elegans has six ASABF-type short peptide molecules that are described in publication: *abf-1* through *abf-6*. Three other homologs have been identified based on sequence similarity and are listed on WormBase (WormBase 2008). GFP reporters for two of the six (ABF-1 and ABF-2) have provided evidence that these peptides are expressed in the pharyngeal lumen, suggesting a role as a digestive enzyme (disrupting the integrity of microbes in order to gain access to their nutritious cellular constituents), as constitutive antimicrobial measures (for example, inactivating pathogenic bacteria in one of their main entry routs) or both. Of interest is that *E. coli*, the worm's standard laboratory diet, seems to be completely immune to ABF-2 (Kato et al. 2002, Pillai et al. 2003). Also, no differential induction of any of the *abf* genes has been measured in *C. elegans*, and for that reason I chose to attempt to measure the worm's expression levels of *abf-1* and *abf-2* in response to challenge by *B. thailandensis.*

The ASABF peptides, including the ABF peptides of *C. elegans*, are defensin-like (Froy 2005, Zhang and Kato 2003) and are technically classified into a class of protein containing Cysteine-Stabilized alpha beta motifs (CSαβ). These peptide molecules contain an α-helix and two β-strands stabilized by 3 to 4 intrachain disulfide bridges

(Froy 2005, Zhang and Kato 2003). They also tend to be positively charged and virtually all contain a secretory signal near the amino-terminal end. This secretory signal is typically cleaved off during post translational modification to yield the final, mature protein. Some of this class of protein also contain a pro region that is cleaved, either along with the secretory signal or in a separate event, to yield the mature protein (Froy 2005, Zhang and Kato 2003). The position of pro regions, the existence and type of introns and the shuffling of exons have been used to discuss and justify the various opinions as to the evolutionary relationships within this class of polypeptide.

With respect to antimicrobial polypeptides in general, there is an enormous and increasing number that have been discovered, from virtually every type of organism known, including bacteria, single celled eukaryotes, fungi, plants and animals (Jenssen et al. 2006). From all these examples, some generalizations can be drawn: antimicrobial peptides tend to be short (<100 aa), they tend to be cationic (though there are exceptions), many function by attacking membranes, they tend to be amphiphilic, and they tend to be stabilized by disulfide bridges.

Pathogens

In this study there were three microbes that I exposed *C. elegans* to: *E. coli* (OP50)*, S. marcescens* (Humboldt soil isolate) and *B. thailandensis* (ATCC#700388). Each behaves like a pathogen toward the worm but to different degrees of virulence and with distinctly different disease progressions.

E. coli (OP50): This is the standard laboratory diet of *C. elegans* and is routinely used as a negative control bacterium in immunological studies using this worm. Even

though this bacterial strain is the standard laboratory food source for the worm, it has some notable pathogenic effects on the worm, especially in older worms or when the bacterium has been grown on rich medium. For example, when OP50 is grown on brain heart infusion agar it kills the worms quite readily with 50% death after 6 days (Garsin et al. 2001). When grown on nematode growth medium, OP50 is far less virulent and the worms live a "normal" life span. However, when grown on *Bacillus subtilis*, worms live about 30% longer than when grown on nematode growth grown OP50, and OP50 is well reported to cause death of old worms through a persistent infection (Ewbank 2006). It is, therefore, possible that the "normal" life expectancy of *C. elegans* is somewhat skewed by the fact that life expectancy quantitations for this worm have generally been done while feeding them on NGM grown OP50.

I chose to use OP50 as my negative control bacterium because under normal nematode growth conditions it is only mildly pathogenic and clearly works well in gaining a baseline of "normal" immune gene expression, as demonstrated by virtually every experimental study done on the subject of *C. elegans* immunity. In addition, I do not have a good replacement for this standard control; in effect, anything I tried to replace it with, for example, *B. subtilis,* would be a deviation from the established negative control microbe (OP50) and would take experimenting in its own right to justify.

S. marcescens (Humboldt soil isolate). Various strains of this Gram negative saprophytic microbe have been known to cause numerous cases of hospital acquired infection for decades. This is interesting because it was originally classified as a non-pathogen. Since that original classification, variant strains of *S. marcescens* have become

known as common causative agents in pneumonia, empyema, meningitis, septicemia, endocarditis, osteomyelitis, peritonitis, sinusitis, urinary tract and wound infections to name the most severe. It typically attacks three groups of people: IV drug users, people with debilitating illnesses and hospital patients who have undergone mildly to heavily invasive procedures. It represents a significant problem for hospitals for at least three reasons: first, various strains contain genome-encoded antibiotic resistance genes and it is readily transformed by multi-drug resistance plasmids that are common in hospitals; second, it has a significantly hydrophobic outer membrane which causes it to readily adhere to (and form biofilms on) plastic, which is extensively used in hospitals for even the most minorly invasive procedures; finally, various strains are significantly resistant to common hospital disinfectants including chlorhexidine, benzalkonium chloride, dimethylbenzyl ammonium chloride and triclosan (Hejazi and Falkiner 1997).

I chose to use this organism in my studies because there is a relatively large body of literature regarding its interaction with *C. elegans* as a host. This literature includes a fairly extensive gene expression study that used microarray, Northern blot analysis, and GFP reporter studies to describe the expression of several genes in the worm under challenge with *S. marcescens* as compared to worms exposed to their normal laboratory diet (Mallo et al. 2002). This bacterium was used as a positive control to demonstrate that the procedures in this study would deliver results consistent with those in publication.

B. thailandensis (ATCC#700388). In contrast to *S. marcescens*, *B. thailandensis* is a relatively little studied pathogen of the worm, with only two experimental publications describing its virulence, and none in the last 5 years (Gan et al. 2002,

O'Quinn et al. 2001). It is nearly identical biologically to the important human pathogen *Burkholderia pseudomallei* (the causative agent of melioidosis) and represents a very recent divergence (evolutionarily speaking) from a common ancestor (Brett et al. 1998, Woo et al. 2002, Yu et al. 2006). This disease has high morbidity and mortality rates in Australia and South East Asia, and the virulence described against *C. elegans* by the human agent is virtually identical to the virulence described for *B. thailandensis*, making the model of *B. thailandensis* challenged *C. elegans* potentially meaningful in the context of the human disease. The big advantage of this model is that *B. thailandensis* is significantly less dangerous for humans than *B. pseudomallei*, though there are some extreme examples of *B. thailandensis* causing disease in humans (Glass et al. 2006).

B. pseudomallei is implicated in as much as 20% of community acquired bacteremias in some areas of Thailand and in one area of Australia it is the leading cause of fatal bacterial pneumonias. *B. pseudomallei* is a Gram negative rod that it is highly resistant to human innate immune mechanisms. It is able to survive the onslaught of microbicidal measures exacted in phagosomes by macrophages, lyse the phagosomes, proliferate in the cytoplasm of host cells, propel itself through the host cell cytoplasm by polymerizing host actin and lyse the host cell by propelling itself through the host cell's outer membrane. When *B. pseudomallei* gains access to tissue cells as an intracellular parasite, it often causes the formation of large multinucleate cells through this action of projecting itself through the membranes that are separating these cells, and thus, causing the adjacent cytoplasms to fuse. Of particular interest with respect to this bacterium's ability to survive in the face of host defenses is its ability to encase itself in an

exoglycocalyx. This doubtlessly protects it not only from recognition by the immune system, but also from the antimicrobial measures exacted by it (Cheng and Currie 2005).

There seems to be a significant innate immune character to this disease, though adaptive immunity clearly cannot be ruled out in determining prognosis. Of great interest is that diseases that affect the adaptive immune system, for example AIDS, do not seem to significantly increase the likelihood of infection by *B. pseudomallei* while diseases which clearly affect the body's ability to mount innate responses, for example diabetes, have great effect on the likelihood of infection. *B. pseudomallei* is resistant to complement, readily infects and persists inside of phagocytic cells (apparently disrupting their expression of important cytokines), is believed by some to easily infect anyone suffering from a myriad of conditions which adversely affect neutrophil function, and it reinfects individuals (multiple times) who are expressing pronounced and highly specific adaptive responses. This being said, activated T-cells are clearly involved in the bodies response and antiserums generated to *B. pseudomallei* LPS have shown a positive effect on patient prognosis in some instances. The available evidence seems to suggest that a large piece of the *B. pseudomallei* strategy in invading a host is to avoid its innate defenses, though this is clearly not the entire picture (Cheng and Currie 2005). This apparent importance of innate immune mechanisms in disease progression makes model innate studies a possibly fruitful endeavor in studying this microbe and the disease it causes.

MATERIALS AND METHODS

Bacterial Strains

Burkholderia thailandensis (ATCC # 700388) was purchased from the American Type Culture Collection (ATCC) (see references). The bacteria were reconstituted at 30 °C as per ATCC instructions. Using aseptic technique, 500 µL of overnight culture was aseptically transferred into 500 µL of sterile 2X freezing solution (65% sterile glycerol, 0.1 M magnesium sulfate, 22 mM Tris-HCl, pH 7.0). This solution was mixed and placed into the -80 °C freezer. The strain was further verified using the 16s ribosomal gene (Table 1).

Serratia marscesens was obtained from Terry Jones in the bacteriology stock room at the Biological Sciences Department at Humboldt State University, Arcata, CA. I created a freezer stock as described above for *B. thailandensis* and further verified this strain by reconstituting it and observing basic colony morphology. Basic verification of strain was made by its characteristic red color when grown at room temperature and further verification was taken as its effect on the *C. elegans* immune system, consistent with those in publication.

Heat killed *E. coli* (that is, non-pathogenic food for the infection experiments) was created by growing 1 L of 24 hour cultures (500 mL in each of two 1 L flasks) of *E. coli* NA22 in Difco nutrient broth at ~35 ºC and ~200 rpm. This culture was then spun at 5000 x g for 15 minutes. The supernatant was decanted and the resulting pellets were resuspended by vortexing in a total volume of 50 mL M9 buffer (to 1L total volume: 6g

Na_2HPO_4, 3g KH_2PO_4, 0.5g NaCl, 1g NH_4Cl, pH to 7.4, autoclave, follow by the addition of 10 mL 0.01M CaCl2). The resuspended bacteria were then heat-killed at 80 ºC for at least 1 hour. The viability of the bacteria were tested following killing.

Worm Strain and Maintenance

C. elegans wild-type (N2) were grown on NGMYT plates (NaCl 1.5g, Bacto-Peptone 1.25g, agar 11.0g, Tryptone 4.0g, Yeast 2.4g, H_2O 500mL, autoclaved 20 min, cooled, followed by addition of 0.5 mL cholesterol [5mg/mL in 95% ethanol], 0.25 mL 1M $CaCl_2$, 0.5 mL 1M $MgSO_4$ and 12.5 mL 1M KH_2PO_4) that were lawned with OP50. They were kept on Petri plates for 3 weeks to a month at a time at 16 ºC. After this time a chunk of agar from the old plate containing worms was aseptically transferred to a fresh NGMYT plate containing a lawn of *E. coli*. This process was repeated indefinitely to maintain the strain.

Infections

Mixed age cultures of worms were raised in liquid culture or on plates. Liquid cultures were grown using 500 mL of M9 buffer supplemented with cholesterol in 2 L flasks at 20 ºC and 100 rpm on a rotary shaker. Twenty five mL of the heat-killed *E. coli* NA 22 was added to these cultures. These cultures were allowed to grow until the population reached approximately 1 million of worms. At this time the cultures were swirled to bring all the worms into suspension and then poured into 50 mL tubes. The tubes were then spun at setting 3 for 5 min in a clinical bench-top centrifuge using a

swinging bucket rotor. The supernatant was carefully removed from the tube using a pipette. The loose pellet was resuspended through inversion in 45 mL of fresh sterile M9 buffer and was spun again for 5 min as above. The supernatant was again carefully removed and the worms were infected with the appropriate pathogen.

Worms raised on plates were raised on NGMYT agar in 100 mm Petri dishes. These worms were raised at 20˚C for approximately 48 hours (until the population was dense and they were beginning to run out of food). These worms were then washed off the plates with 5 mL of sterile M9 buffer. The buffer was rinsed over the plates 5 to 10 times, and was then transferred to 50 mL tubes as described above for liquid cultures. The worms in this buffer were then spun as described above but were instead washed twice with 45 mL of sterile M9 buffer before infection with appropriate pathogens.

Infections in M9 were carried out by growing 250 mL bacterial (*E. coli* and *S. marcescens* or *B. thailandensis*) cultures in Difco nutrient broth with ~200 rpm shaking at 35 ºC for 24 hours. These cultures were then transferred to 300 mL centrifuge tubes and spun at 5000 x g for 15 min. The supernatant was decanted and the pellet was resuspended in 50 mL of M9 through vortexing. The optical density of the resulting solutions was measured at 600 nm and infection cultures were generated such that the optical density of each bacterial species was 0.44 in each of the infections. The final volume within each set of infections (i.e. controls vs. experimentals) was 10 mL. To each culture was added 100 µL of 5% cholesterol (described above). These infections were then allowed to proceed at 20 ºC for 24 to 48 hours with shaking at 100 rpm in a 50 mL flask.

Following the infection, the worms were transferred to 15 mL tubes and spun down for 5 min as described above. The pellet was washed twice by resuspension in M9 followed by respinning. Following the final spin, the pellet of worms was carefully drawn into a pipette and added dropwise to a 50 mL tube containing liquid nitrogen. This created flash frozen worm pellets, which were stored until further use at -80 ºC.

To prep these pellets for RNA isolation they were crushed using a mortar and pestle under cryogenic conditions (liquid nitrogen was placed into the mortar and the nose of the pestle was frozen in a bath of liquid nitrogen prior to grinding). The pulverized worm pellets were then transferred to Eppendorf tubes sitting in a bath of liquid nitrogen using a microspatula also frozen in liquid nitrogen. These Eppendorf tubes containing pulverized worms were then stored at -80 ºC until their usage in RNA isolation.

RNA Isolations

RNA isolations were performed using the RNAqueous®-4PCR Kit from Ambion (Foster City, CA). The isolations were done using the protocol provided with the kit using the volumes described for $1x10^7$ cells. Lysis buffer was added directly to tubes containing pulverized worms (above), and the frozen worm pellets were then thawed in the lysis buffer prior to continuing the isolation protocol.

Genes and Primers

All primers used are shown in Table 1. Primers were created using Vector NTI Advance 10, a software package available from Invitrogen (Carlsbad, CA). The cDNA sequences for the genes used (see introduction) were obtained either from WormBase or NCBI (see references). The pGEM circular plasmid sequence is shown in appendix 1. All primers were extensively tested *in silico* for homo and heterodimers as well as hairpins. In addition, all primers for real time PCR were generated to have replicons of under 200 bp. For real-time reactions done with high statistical stringency (see below) experimental and reference primer sets were generated to have replicons of a length within 10 bp of each other. For example, if the replicon for the reference gene primer set is 130 bp, then the experimental gene primer set was generated to be within 10 bp of this length. The 16S primers for *B. thailandensis* were created by aligning *E. coli*, *S. marcescens,* and *B. thailandensis* 16S DNA sequences (Thompson et al. 1994) and finding uncommon segments within. These primers were then tested as above for dimers, etc.

Handling of RNA Samples

All procedures involving RNA samples were carried out using aseptic technique. RNA samples were isolated into sterilized virgin plastic (that is, new and never previously used) Eppendorf tubes. All reagents were either provided in kits or were prepared in glassware that had been baked at 200 ºC

Table 1. Genes and primers used in PCR reactions. All primers were generated using Vector NTI Advance and were tested *in silico* for favorable hairpins, intra- and inter-chain dimers. In addition, primers generated for real-time reactions were designed to have a replicon of < 200 bp length. The primers used in high stringency real-time PCR reactions were designed to have replicons within 10 bp in length of one another

Gene	Primer sequence
B. thailandensis 16S	5'-AAAGAAATCATCCTGGC-3'
	5'-CGTTACTAAGGAAATGAATC-3'
lys-1	5'-GAACTGCCTCAAGACATCCAGATA-3'
(low and high stringency rxns)	5'-GAGTCATGTAGACCTCAATTCCCA-3'
nlp-29	5'-TTGTTCTTGTCGTCCTTCTCG-3'
	5'-TTACTTTCCCCATCCTCCATAC-3'
abf-1	5'-ATGCTTTACTTCTGCCTTCTCC-3'
	5'-AGTCCTTGTGCGATCCTCTG-3'
abf-2	5'-ATGTTCGTCCGTTCCCTTT-3'
(low stringency rxns)	5'-GACCGCTTCGTTTCTTGC-3'
lys-7	5'-AAAC TCCTGCCAACTTCAA-3'
	5'-ATCTTCCCGTCTTCTTCAAC-3'
lys-8	5'-CTTTCGCTGTTGATTTGTC-3'
	5'-AGTATTGCAGGAGTTGGTGT-3'
abf-2	5'-AAAAGCGGCTCAGGGGTTGT-3'
(high stringency rxns)	5'-CACCAAGTGGAATATCTCCTCCTC-3'
rla-1	5'-TTCCTCCTTTGGCTCCTCCT-3'
	5'-ATATGAAGAACCTCATCACTTCTGTCTC-3'
pGEM	5'-CCGACAGGACTATAAAGATACCAG-3'
(for standard curves)	5'-CTACAGCGTGAGCTATGAGAAAGC-3'

.

for at least 24 hours. The only materials that came into contact with the samples after isolation were RNase free reagents provided with kits or prepared by me using diethylpyrocarbonate (Ausubel et al 1995), RNase-free virgin plastic PCR tubes and virgin plastic aerosol filter micro pipette tips. During measurement of RNA concentrations, the RNA samples were taken out of the freezer and placed on ice. They were allowed to sit on ice for 10 minutes. They were then spun at maximum velocity in an Eppendorf desktop centrifuge for approximately 10 seconds. After this they were gently agitated by flicking with a finger to slightly vortex and dislodge any remaining ice. The samples were then placed on ice again for another time period of up to 10 minutes. During this time they were checked frequently for completed thawing. This process was repeated until the sample was completely thawed. When the samples had completely thawed they were spun one additional time at maximum velocity for approximately 10 seconds. They were then immediately quantified (below) and placed back at -80 ºC.

Quantification of RNA

RNA samples were quantified on a Beckman DU 640 spectrophotometer at 230 nm, 260 nm and 280 nm. The average of 4 readings was used to determine the final concentration. The 260/280 ratio and 260/230 ratio were used to determine protein and guanadinium isothiocyanate contamination, respectively, in the samples. In addition, samples were usually quantified at full concentration to avoid the error associated with dilutions.

Real-Time PCR

The real-time PCR reactions were carried out using iScript One Step Real-Time PCR reagents from Bio-Rad, Inc. (see references). Reaction cocktails were set up such that individual reactions were calculated to have 12.5 µL of iScript PCR supermix, 1 µL both of forward and reverse primer, 0.5 µL of reverse transcriptase, identical quantities of RNA and nuclease free water such that the final volume equaled 25 µL. The cocktail was prepared for a total of 4 reactions. The RNA was added second to last and following this the slurry was mixed by pipetting several times up and down (~80 µL). One 20 µL reaction was then removed and put into a thin-walled, nuclease-free PCR tube. This was the no reverse transcriptase control. After this, reverse transcriptase (2 µL) was added to the slurry and the slurry was again mixed by pipetting up and down 5-7 times. The cocktail was then aliquoted into three 20 microliter reactions. These were the experimental reactions.

The thermocycle regime was as follows: 50 ºC for 10 minutes; 95 ºC for 4 minutes; then 40-60 cycles of 95 ºC for 20 sec, 2 degrees lower than the lowest Tm of the primer sets for 30 seconds and 70 ºC for 45 seconds. The real-time data (that is, the fluorescence readings) were taken at the annealing step. Following this thermocycle regime a melt curve was taken. The samples were heated up to 95 ºC for one minute and then brought to 4 ºC. The temperature was then increased by 1/2 ºC every ten seconds until the samples were at 95 ºC, with a fluorescence reading being taken at each

temperature step. The fluorescence data from both above processes were compiled by the iCycler software into amplification curves and melt curves, respectively.

Quantification of Dynamic Range of the iCycler Detection System with Standard Curves

Standard curves were generated using known concentrations of pGEM circular vector in dilution series. The dilution series was an order of magnitude more dilute for each dilution (i.e. 1, 1/10, 1/100, etc.). The standard curve reactions were created by mixing real time PCR reactions as described above with the exception that each reaction contained pGEM DNA instead of worm RNA. These reactions were run using the same thermocycle regime as described above minus the melt curve.

High Statistical Stringency Real-Time PCR

To obtain expression data of high statistical stringency I used the method described by Marino et al (2003). Briefly, six biological replicates of each gene and condition to be tested are run in parallel and compared to six biological replicates of a reference gene also under each condition. The RNA samples generated from the treatments are then equalized in concentration and added in equal volume to separate real time PCR reactions. These reactions are all run in parallel and the resulting amplification data are processed as described by Marino et al (2003).

Worms were exposed to *B. thailandensis* (ATCC) and *E. coli* (OP50), and *lys-1, abf-2* and *rla-1* (large ribosomal subunit gene) were used as the two experimental genes and reference gene, respectively. Following the infection protocol described above, the

worm pellets were frozen in liquid nitrogen and transferred to Eppendorf tubes for storage at -80 ˚C. In this procedure, worm pellets were not ground with a mortar and pestle. Instead, lysis buffer was added directly to the Eppendorf tubes containing the frozen pellets. These tube were then clasped in hand and inverted until the frozen pellet had thawed. The tubes were then placed into a Eppendorf desktop centrifuge and spun at high speed for ~30 seconds. The pellet of worms was then crushed in lysis buffer using the cotton-free end of a Q-tip. All the resulting RNA samples were equalized in concentration prior to addition to PCR reaction slurries.

Bioinformatics Analysis

Because I observed a pointed down-regulation of *abf-2* expression in response to specific infection conditions I performed a series of bioinformatics analyses on this class of peptide. In order to see if there are any human sequences that are distantly related ASABF-type antimicrobial peptides, I did low stringency searches of the human genome using BLAST analysis (National Center For Biotechnology Information 2007) of *abf-2*, and ran a series of protein property prediction algorithms on any exonic matches found. In addition, to see if it is common for short predicted proteins in the human genome to meet the same theoretical parameters as known antimicrobial peptides, I selected a segment of human chromosome 2 at approximately 124.5 million bp on the physical map that is rich in Gnomon-predicted (National Center For Biotechnology Information 2003) gene sequences (Figure 1), and selected 130 short predicted proteins to analyze.

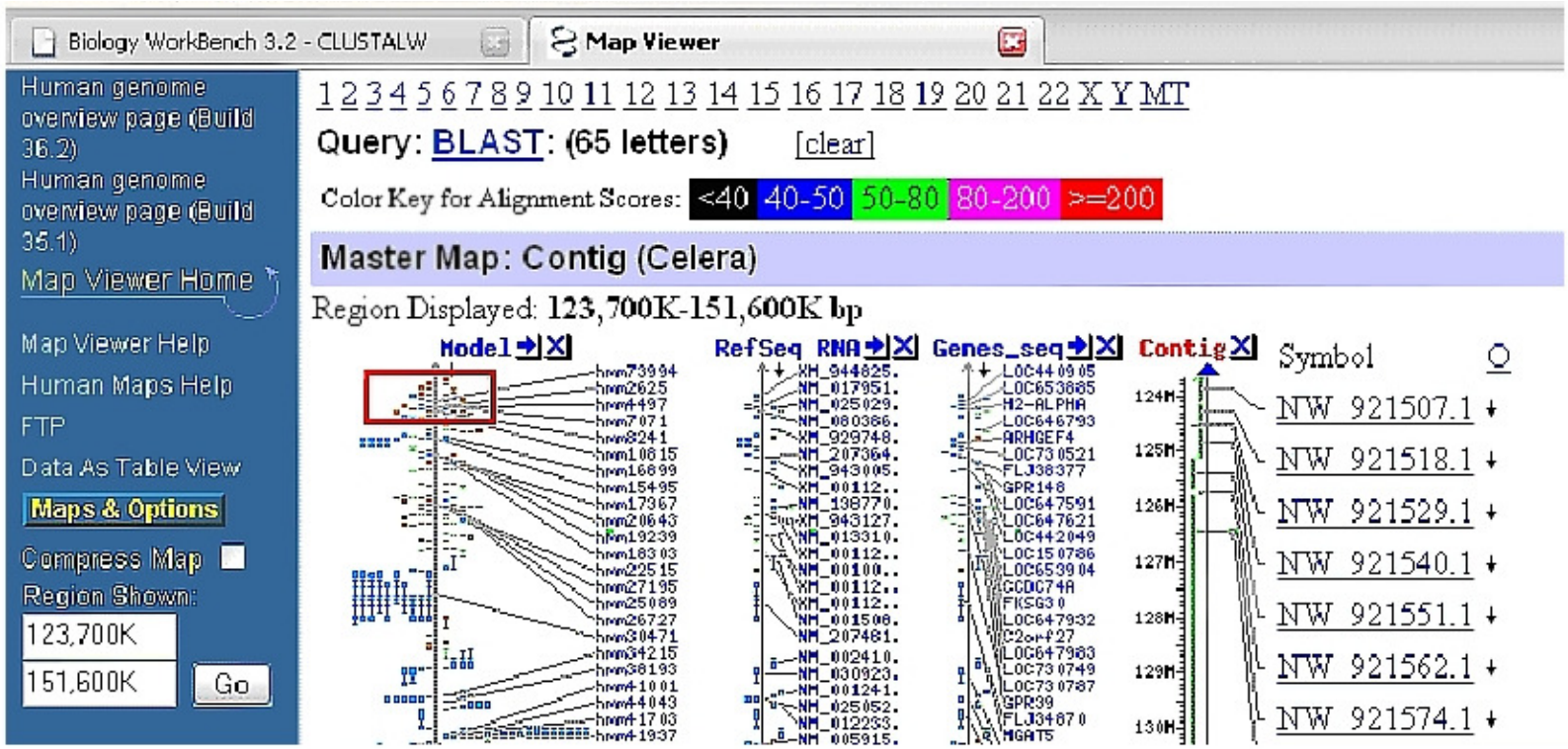

Figure 1 Genomic map of human chromosome 2 showing the general location of sequences harvested for bioinformatics analysis (red box).

For BLAST analysis, the *abf-2* mRNA sequence was obtained from WormBase (see references) and was pasted into the BLAST search field for the human genome. The stringency was set to the lowest possible level and the program "BLASTN: compare nucleotide sequences" was selected. The protein sequences of exonic BLAST hits were pasted into Biology Workbench, available online from the UC San Diego Super Computing Center (Biology Workbench 2003), and were subjected to the following *in silico* analyses: Isoelectric point estimation (Toldo 1995), transmembrane segment prediction (Persson and Argos 1994) and Kyte-Doolittle hydropathy plots (Kyte and Doolittle 1982). In addition, the length in amino acids was noted, the number of cysteine residues was noted and alignments were made of selected sequences to the ABF-2 and several human Defensin-like protein sequence (Thompson et al. 1994). As a final analysis, the sequences were checked for secretion signals and cleavage points using SignalP 3.0 (Bendtsen et al. 2004)

Gnomon predicted sequences harvested from chromosome 2 were subject to the same tests as above. The 130 sequences harvested were selected due to their short length and no predicted function. Specifically, sequences of under 200 amino acids were selected that did not have suspected homology, based on sequence, to proteins of known function. For example, a sequence of under 200 amino acids that was listed as showing significant similarity to alpha-tubulin was rejected. Only short predicted peptides of no known function were selected.

RESULTS

Standard Curves and the iCycler Dynamic Range

Figure 2 shows amplification data from triplicate reactions run with eight differing concentrations of pGEM, all one order of magnitude different compared to adjacent triplicates. These data are also shown in the form of threshold values in Table 2, and they are as follows: CT = 10.5 for 54.9 pg/µL, CT = 13.5 for 5.49 pg/µL, CT = 16.6 for 5.49 pg/µL, CT = 20.7 for 549 fg/µL, CT = 24.5 for 54.9 fg/µL, CT = 24.5 for 5.49 fg/µL, CT = 27.9 for 549 zg/µL, CT = 28.9 for 54.9 zg/µL, CT = 30.1 for 5.49 zg/µL. The logarithmic separation of CT values between differing pGEM concen-trations stops being apparent starting from a concentration of 549 zg/µL to 5.49 zg/µL. The average of the difference between threshold cycles for pGEM concentrations, excluding the lowest three, is 3.5 cycles per 10 fold difference in concentration.

Table 2 also shows amplification data in the form of threshold cycle values for each of triplicate reactions run with five differing concentrations of pGEM vector. The average threshold values for the standard concentrations in this series are CT = 8.77 for 61.1 pg/µL, CT = 11.93 for 6.11 pg/µL, CT = 15.03 for 611 fg/µL, CT = 18.57 for 61.1 fg/µL and CT = 21.50 for 6.11 fg/µL. The average change in threshold cycle for pGEM concentrations one order of magnitude different is 3.18. For this concentration range there is no loss of logarithmic separation, indicating that these concentrations are within the linear range of the BioRad iCycler.

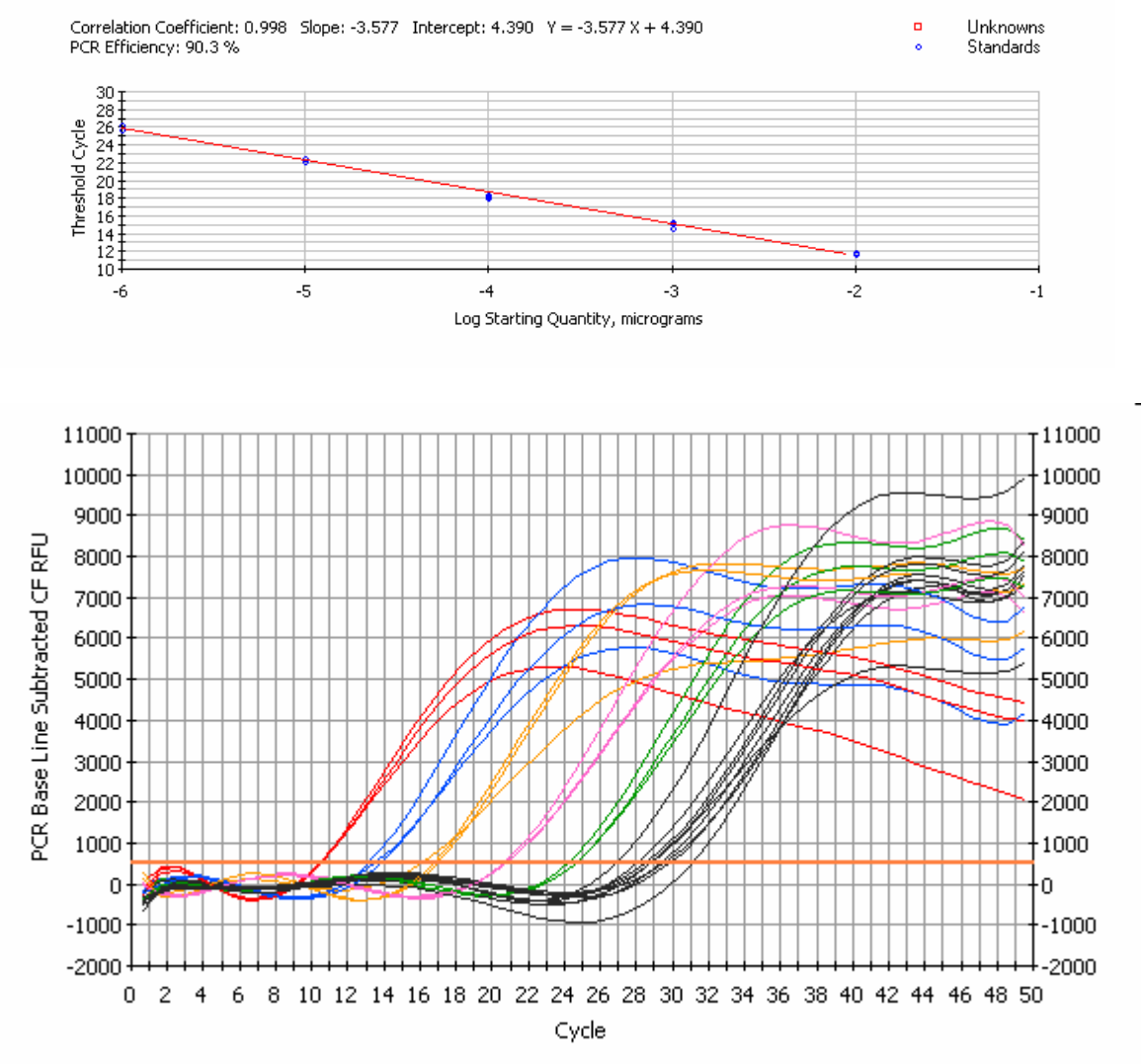

Figure 2 Amplification curves showing real-time PCR reactions run using known concentrations of circular pGEM plasmid. Reactions were run in triplicate with each triplicate containing a different dilution of pGEM in a 1/10 dilution series. The concentrations are listed below. The upper plot shows the standard curve based on these reactions and the lower plot shows the amplification curves.

(—) 54.88 pg/µL
(—) 5.488 pg/µL
(—) 548.8 fg/µL
(—) 54.88 fg/µL
(—) 5.488 fg/µL
(—) 548.8 to 5.488 zg/µL

Table 2 Threshold values for reactions run using known concentrations of pGEM vector in 1/10 dilution series for the generation of standard curves. There were two non-identical series run with each concentration within a series run in triplicate. Standard curves were generated from these data to determine dynamic range and amplification parameters

Threshold values for first series of standard rxns:

Concentration	Threshold Cycle	Concentration	Threshold Cycle	Concentration	Threshold Cycle
61.1 pg/µL	8.4	611 fg/µL	15.4	6.1 fg/µL	21.2
61.1 pg/µL	9.1	611 fg/µL	15	6.1 fg/µL	21.8
61.1 pg/µL	8.8	611 fg/µL	14.7	6.1 fg/µL	N/A
6.11 pg/µL	11.7	61.1 fg/µL	18.1	--	--
6.11 pg/µL	12	61.1 fg/µL	18.2	--	--
6.11 pg/µL	12.1	61.1 fg/µL	17.8	--	--

Threshold values for second series of standard rxns:

Concentration	Threshold Cycle	Concentration	Threshold Cycle	Concentration	Threshold Cycle
54.88 pg/µL	10.5	54.88 fg/µL	20.8	54.88 zg/µL	29.4
54.88 pg/µL	10.4	54.88 fg/µL	20.6	54.88 zg/µL	28.5
54.88 pg/µL	10.6	54.88 fg/µL	20.7	54.88 zg/µL	28.8
5.488 pg/µL	13.5	5.488 fg/µL	24.2	5.488 zg/µL	29.6
5.488 pg/µL	13.1	5.488 fg/µL	24.6	5.488 zg/µL	31
5.488 pg/µL	13.8	5.488 fg/µL	24.6	5.488 zg/µL	29.8
548.8 fg/µL	16.1	548.8 zg/µL	27.5	--	--
548.8 fg/µL	17	548.8 zg/µL	28.2	--	--
548.8 fg/µL	16.7	548.8 zg/µL	26.4	--	--

S. marcescens Exposures In M9

A representative chart for the reactions run using RNA from worms exposed to *Serratia marcescens* in M9 for 48 hours is shown in Figures 3. These data are also shown in Table 3. These reactions were all run with *lys-1* primers. The difference between amplification C_T (infection vs. control) is 2.6 which corresponds to a 6.1 fold mRNA copy number increase in *S. marcescens* infected worms. The no reverse transcriptase controls did not cross the threshold during the course of the reaction. The melt curve for these reactions (Figure 3) shows a single peak at ~81 °C, suggesting a single, identical product in experimental and control reactions.

The difference between amplification C_T in the second replication of this infection is 2.1 (Table 3), which corresponds to a 4.3 fold mRNA copy number increase in *S. marcescens* infected worms. The no reverse transcriptase controls cross the threshold more than 18 cycles later than the experimental reactions indicating a >250,000 fold difference in mRNA copy number compared to oligomeric DNA in these reactions. The melt curve (data not shown) showed a single peak at ~81 °C in the experimental reactions, and two slightly different peaks between the no reverse transcriptase reactions, indicating slightly disparate products in the control reactions.

The amplification data for the third replication of these exposures is shown in Table 3. The difference between amplification C_T in this third replication is 1.8 which corresponds to a 4.3 fold mRNA copy number increase in *S. marcescens* infected worms. The no reverse transcriptase controls did not cross the threshold.

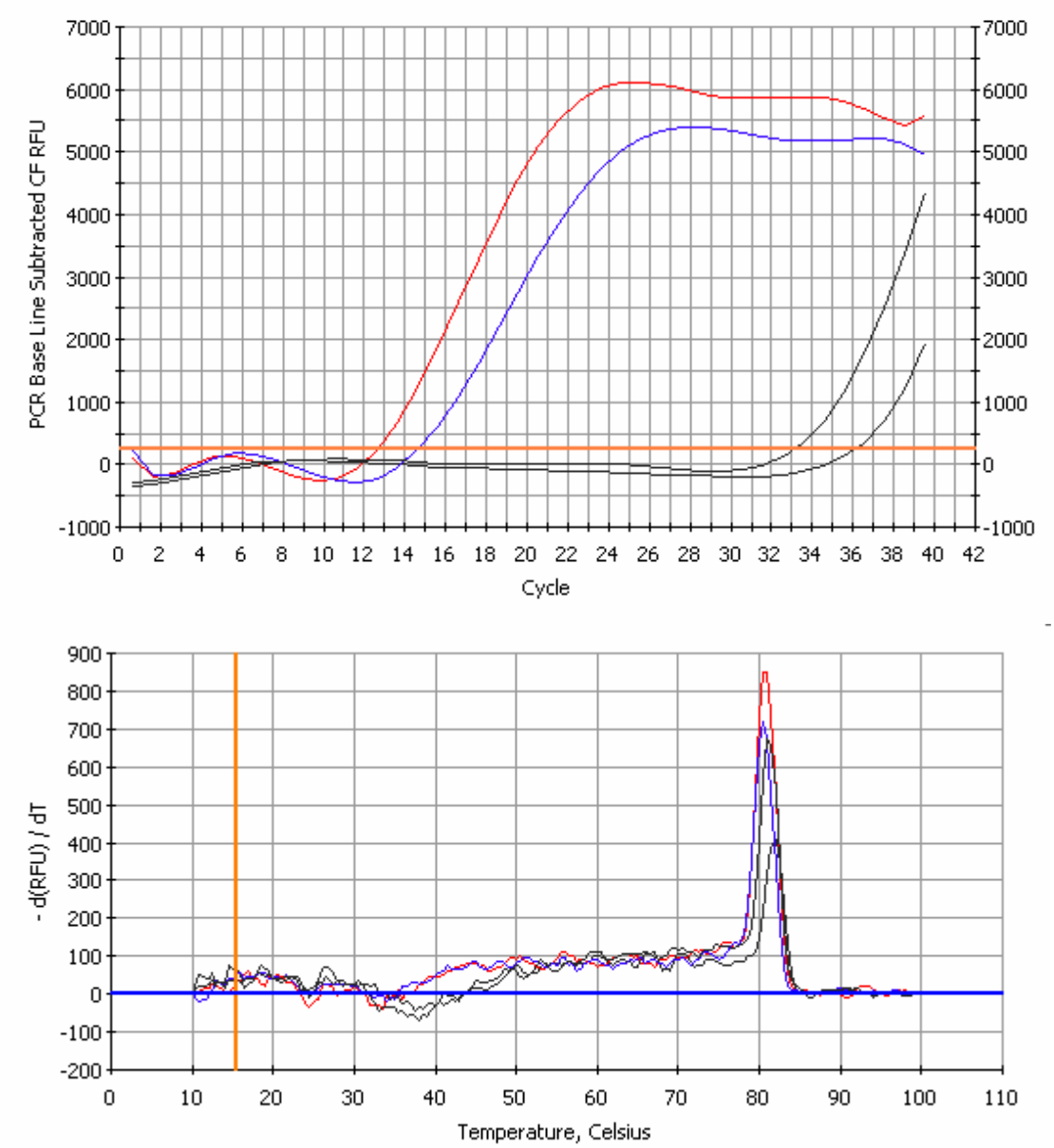

Figure 3 Real-time PCR reactions containing RNA from the second replication of worms exposed to *S. marcescens* and *E. coli* OP50 in M9 for 48 hours. These reactions were run using *lys*-1 primers. The upper graph shows amplification curves and the lower graph shows melt curves.
(—) *S. marcescens* exposed
(—) *E. coli* exposed
(—) No reverse transcriptase control

Table 3 PCR threshold cycles for three replications of infections and controls using S. *marcescens* as a pathogen. The RNA samples run in these reactions were obtained from worms exposed for 48 hours.

Threshold cycles for first reactions with *lys-1* primers:

Sample	Threshold cycle	Sample	Threshold cycle
S. marcescens exposed	24.4	*E. coli* exposed	27
No reverse trans	N/A	No reverse trans	N/A

Threshold cycle for second reactions with *lys-1* primers:

Sample	Threshold cycle	Sample	Threshold cycle
S. marcescens exposed	12.6	*E. coli* exposed	14.7
No reverse trans	36.1	No reverse trans	33.1

Threshold cycles for third reactions with *lys-1* primers:

Sample	Threshold cycle	Sample	Threshold cycle
S. marcescens exposed	13.7	*E. coli* exposed	15.5
No reverse trans	N/A	No reverse trans	N/A

Burkholderia thailandensis Exposures In M9

A representative graph showing data for reactions run with RNA from worms exposed to *B. thailandensis* in M9 for 48 hours is shown in Figure 4. These reactions were run using primers for *lys-1,* and Table 4 contains data for all replications of this exposure. The difference in threshold value between the first two treatments is 0.8, which represents a 74% mRNA copy number increase in *B. thailandensis* infected worms. The no reverse transcriptase controls did not cross the threshold, and there was no melt curve performed in this reaction set.

The difference in threshold value between the second set of these treatments is 1.4 which represents a 2.6 fold mRNA copy number increase in *B. thailandensis* infected worms (Table 4). The no reverse transcriptase controls did not amplify. The melt curve (Figure 4) shows a single peak in both experimental reactions at ~81 °C, indicating a single product in these reactions.

The third replication of these exposures was run in triplicate. The average difference in threshold value between the infected vs. control treatments is 1.6, which represents a 3.0 fold mRNA copy number increase in *B. thailandensis* infected worms. A two tailed T-test between the two triplicate series in Table 4 returns a value of P=0.0030. The no reverse transcriptase controls did not cross the threshold, and the melt curve (data not shown) showed a single peak for all reactions at ~81 °C.

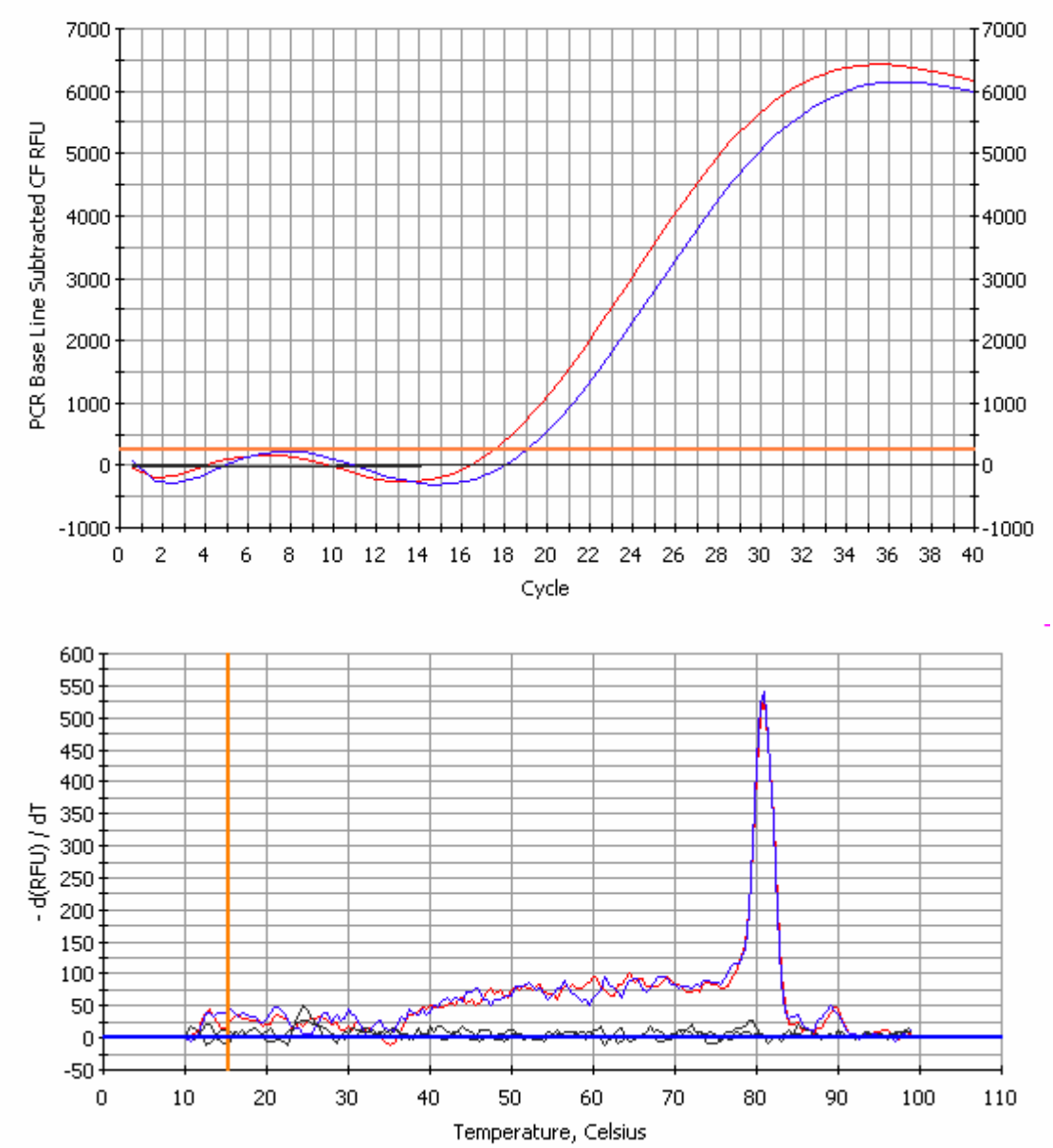

Figure 4 Real-time PCR reactions containing RNA from the second replication of worms exposed to *B. thailandensis* ATCC 700388 and *E. coli* OP50 in M9 for 48 hours. These reactions were run using *lys*-1 primers. The upper graph shows amplification curves and the lower graph shows melt curves.
(—) *B. thailandensis* exposed
(—) *E. coli* exposed
(—) No reverse transcriptase control

Table 4 PCR threshold cycle values for reactions run using RNA from B. thailandensis exposures. Worms were exposed for 48 hours in rich medium. Only the final reactions in the group of replicates were run in triplicate

Threshold cycles for first reaction with lys-1 primers:

Sample	Threshold cycle	Sample	Threshold cycle
B. thailandensis exposed	33.9	E. coli exposed	34.7
No reverse trans	N/A	No reverse trans	N/A

Threshold cycles for second reaction with lys-1 primers:

Sample	Threshold cycle	Sample	Threshold cycle
B. thailandensis exposed	17.6	E. coli exposed	19.0
No reverse trans	N/A	No reverse trans	N/A

Threshold cycles for third reaction with lys-1 primers:

Sample	Threshold cycle	Sample	Threshold cycle
B. thailandensis exposed	25.8	E. coli exposed	26.9
B. thailandensis exposed	25.1	E. coli exposed	27.4
B. thailandensis exposed	25.6	E. coli exposed	27.1
No reverse trans	N/A	No reverse trans	N/A

.

Worms Exposed To Conditioned Medium

Expression levels of *lys-1*.

A representative graph for the reactions run using *lys-1* primers against RNA from worms exposed to conditioned medium is shown in Figure 5. All replications of this reaction are shown in Table 5 and were run in triplicate. The average C_T value for the first replication containing RNA from *B. thailandensis* treatments is 16.6. That for reactions containing RNA from *E. coli* treatments is 17.2. This represents a 62% mRNA copy number increase in *B. thailandensis* conditioned worms (P=0.10). The no reverse transcriptase controls cross the threshold much later than the experimental reactions. The melt curve (data not shown) showed a single peak for all reactions at ~81 °C.

The average C_T value for the second replication of these reactions containing RNA from *B. thailandensis* treatments is 16.9, and the average for reactions from *E. coli* treatments is 17.1, corresponding to a 15% mRNA copy number increase in *B. thailandensis* conditioned worms (P=0.19). The no reverse transcriptase controls amplified at least 5 cycles later than the experimental reactions, representing a 32 fold difference in gene copy number between oligomeric DNA and mRNA in the *B. thailandensis* conditioned RNA sample. The melt curve (Figure 5) shows one peak from one no reverse transcriptase control at ~76 °C. All other reactions show an identical peak at ~81 °C.

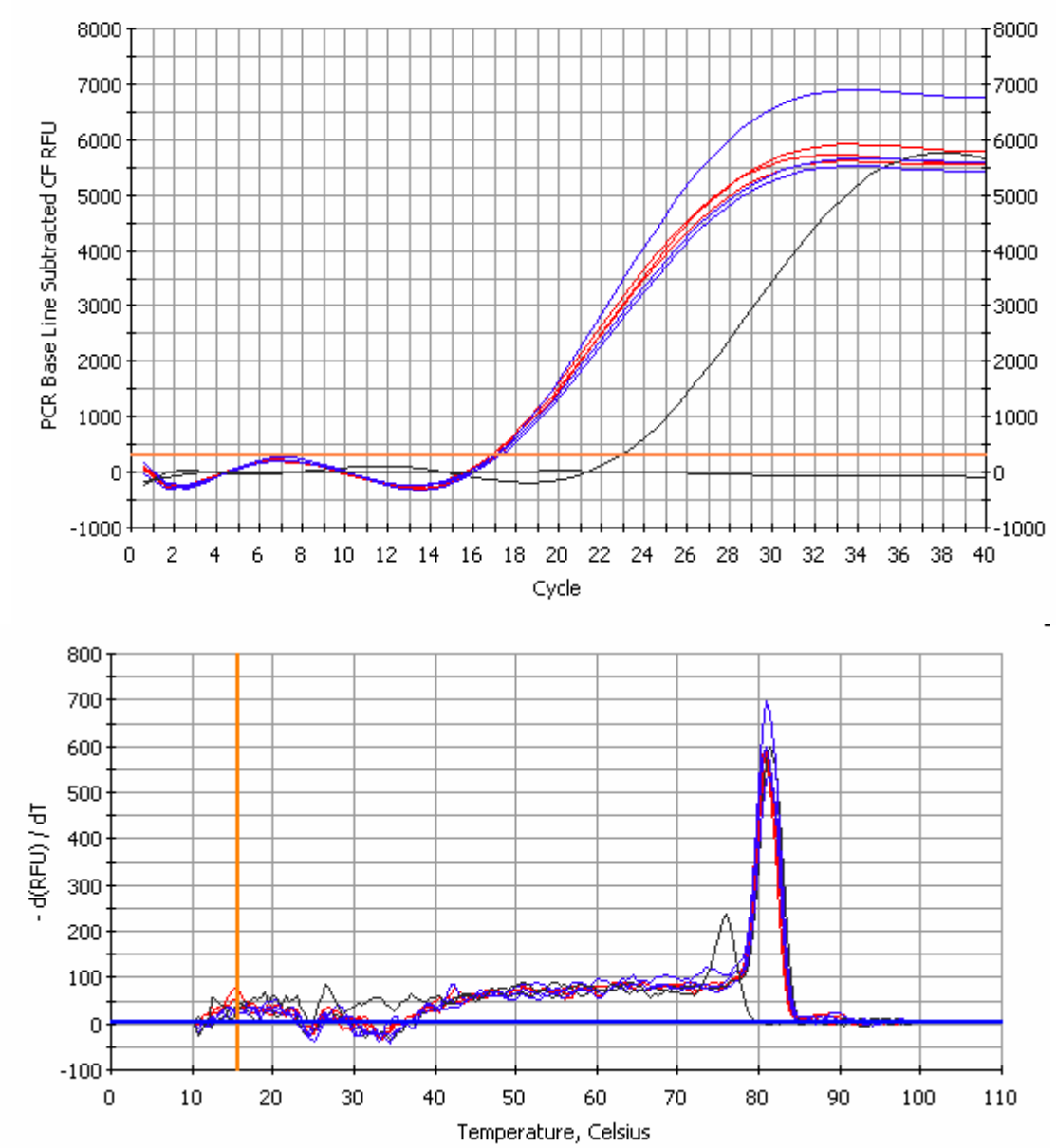

Figure 5 Real-time PCR reactions containing RNA from the second replication of worms exposed to *B. thailandensis* ATCC 700388 and *E. coli* OP50 filtered medium for 24 hours. These reactions were run using *lys-1* primers. The upper graph shows amplification curves and the lower graph shows melt curves.
(—) *B. thailandensis* exposed
(—) *E. coli* exposed
(—) No reverse transcriptase control

Table 5 Real-Time PCR threshold values for reactions run using RNA from worms exposed to *B. thailandensis* for 24 hours. All reaction were run in triplicate.

Threshold cycles for first reaction with *lys-1* primers:

Sample	Threshold cycle	Sample	Threshold cycle
B. thailandensis exposed	16.5	*E. coli* exposed	17.3
B. thailandensis exposed	16.4	*E. coli* exposed	17.7
B. thailandensis exposed	16.8	*E. coli* exposed	16.7
No reverse trans	27.1	No reverse trans	29.8

Threshold cycles for second reaction with *lys-1* primers:

Sample	Threshold cycle	Sample	Threshold cycle
B. thailandensis exposed	17.1	*E. coli* exposed	17.0
B. thailandensis exposed	16.9	*E. coli* exposed	17.1
B. thailandensis exposed	16.8	*E. coli* exposed	17.2
No reverse trans	22.9	No reverse trans	47.7

Threshold cycles for third reaction with *lys-1* primers:

Sample	Threshold cycle	Sample	Threshold cycle
B. thailandensis exposed	15.7	*E. coli* exposed	16.5
B. thailandensis exposed	15.6	*E. coli* exposed	16.2
B. thailandensis exposed	15.7	*E. coli* exposed	16.2
No reverse trans	26.4	No reverse trans	N/A

.

The average C_T value for the third replication of reactions containing RNA from *B. thailandensis* treatments is 15.7, and the average for reactions from *E. coli* treatments is 16.3. This corresponds to a 60% mRNA copy number increase in *B. thailandensis* conditioned worms (P=0.0039). The no reverse transcriptase control for the *B. thailandensis* exposed treatments crosses the threshold at 26.4, a 10.7 cycle difference as compared to the average C_T value for the experimental reactions run with this RNA sample (mRNA copy number >1,600 x DNA copy number), suggesting trace oligomeric DNA contamination. The melt curve (data not shown) showed a single peak for the experimental reactions at ~81 °C and a slightly different peak (~82 °C) for the no reverse transcriptase control reaction that amplified.

Expression levels of *lys-7*.

A representative graph for reactions run using *lys-7* primers against RNA from two replications of conditioned medium exposures is shown in Figure 6. The amplification data for both replications of these exposures is shown in Table 6, and all reactions were run in triplicate. The average threshold value for the first replication of *B. thailandensis* treatments was 19.0 and the average for the *E. coli* treatments was 18.7, corresponding to a 23% mRNA copy number decrease in *B. thailandensis* conditioned worms (P=0.28). The no reverse transcriptase controls cross the threshold much later than the experimental reactions, and the melt curve (data not shown) showed identical peaks for all reactions at ~83 °C.

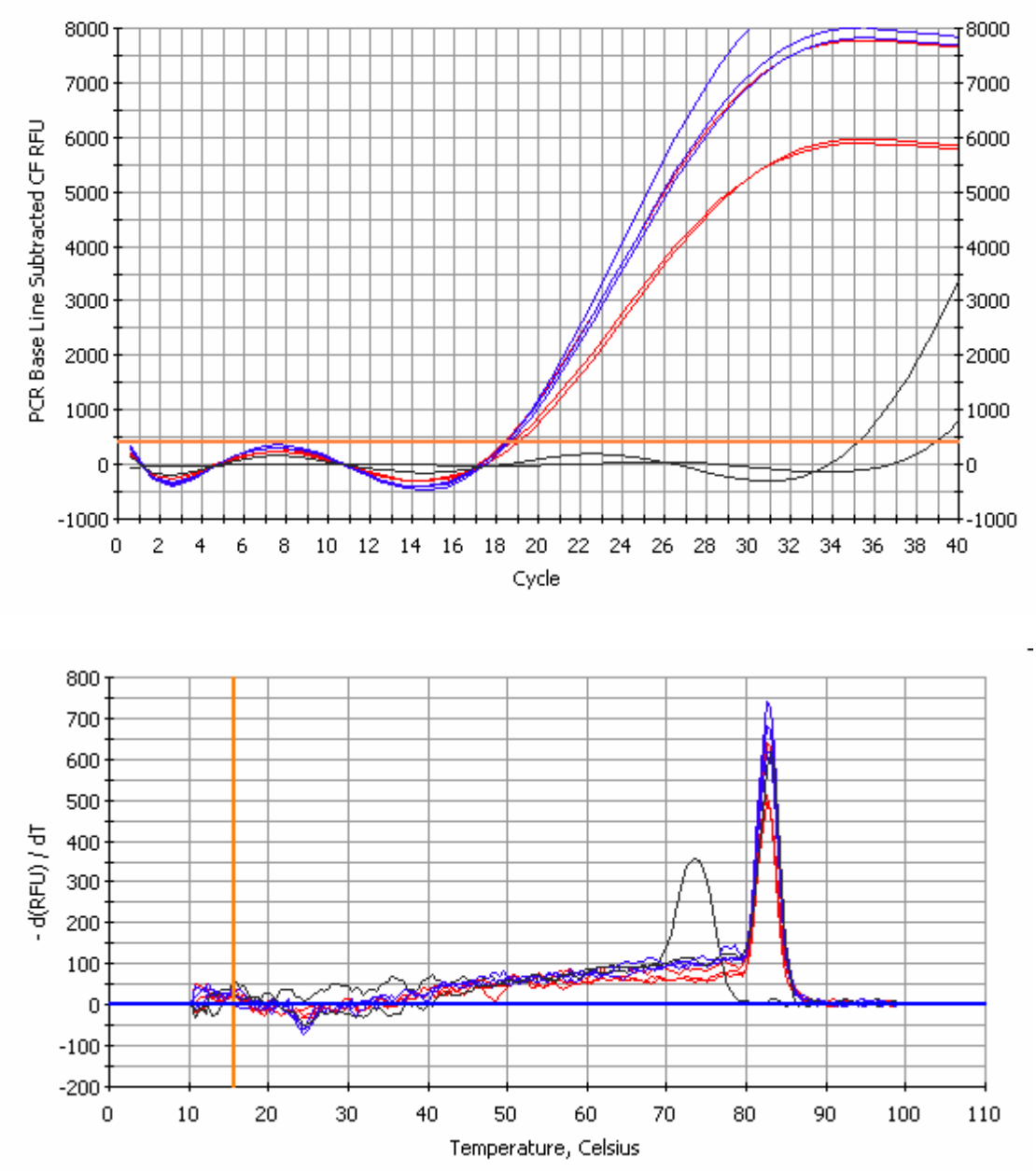

Figure 6 Real-time PCR reactions containing RNA from the second replication of worms exposed to *B. thailandensis* ATCC 700388 and *E. coli* OP50 filtered medium for 24 hours. These reactions were run using *lys-7* primers. The upper graph shows amplification curves and the lower graph shows melt curves.
(—) *B. thailandensis* exposed
(—) *E. coli* exposed
(—) No reverse transcriptase control

Table 6 PCR threshold cycles for 2 replications of reactions run using RNA from worms exposed to *B. thailandensis* conditioned medium for 24 hours. Each reaction was run in triplicate.

Threshold cycles for first reaction with *lys-7* primers:

Sample	Threshold cycle	Sample	Threshold cycle
B. thailandensis exposed	18.9	*E. coli* exposed	18.8
B. thailandensis exposed	19.1	*E. coli* exposed	18.4
B. thailandensis exposed	18.9	*E. coli* exposed	19
No reverse trans	35	No reverse trans	36.5

Threshold cycles for second reaction with *lys-7* primers:

Sample	Threshold cycle	Sample	Threshold cycle
B. thailandensis exposed	18.4	*E. coli* exposed	18.5
B. thailandensis exposed	18.7	*E. coli* exposed	18.6
B. thailandensis exposed	19.0	*E. coli* exposed	18.5
No reverse trans	38.9	No reverse trans	35.2

The average C_T value for the second replication of *B. thailandensis* treatments is 18.7, and the average for the *E. coli* treatments is 18.5, representing a 15% mRNA copy number increase in *B. thailandensis* conditioned worms (P=0.40). The no reverse transcriptase controls cross the threshold much later than the experimental reactions. The melt curve (Figure 6) shows a peak at ~74 °C for one of the no reverse transcriptase controls, indicating a non-specific product, and a single peak for all other reactions at ~83 °C.

Expression levels of *lys-8.*

A representative graph showing reactions run using *lys-8* primers against RNA from conditioned medium exposures is shown in Figure 7. The data for all replications of these reaction are shown in Table 7, and all reactions were run in triplicate. The average C_T value for the first replication of *B. thailandensis* treatments is 16.6 and the average for *E. coli* treatments is 17.4, corresponding to a 74% mRNA copy number increase in *B. thailandensis* conditioned worms (P=0.054). It should be noted that one outlier was left out of this calculation (*B. thailandensis* triplicate #3) as it is clear that reverse transcriptase did not make it into this reaction. The no reverse transcriptase controls amplified many cycles later than the experimental reactions indicating no significant quantities of oligomeric DNA contamination in the respective RNA samples. The melt curve (data not shown) shows one peak for one of the no reverse transcriptase controls at ~84 °C and another peak at ~85 °C for all other reactions.

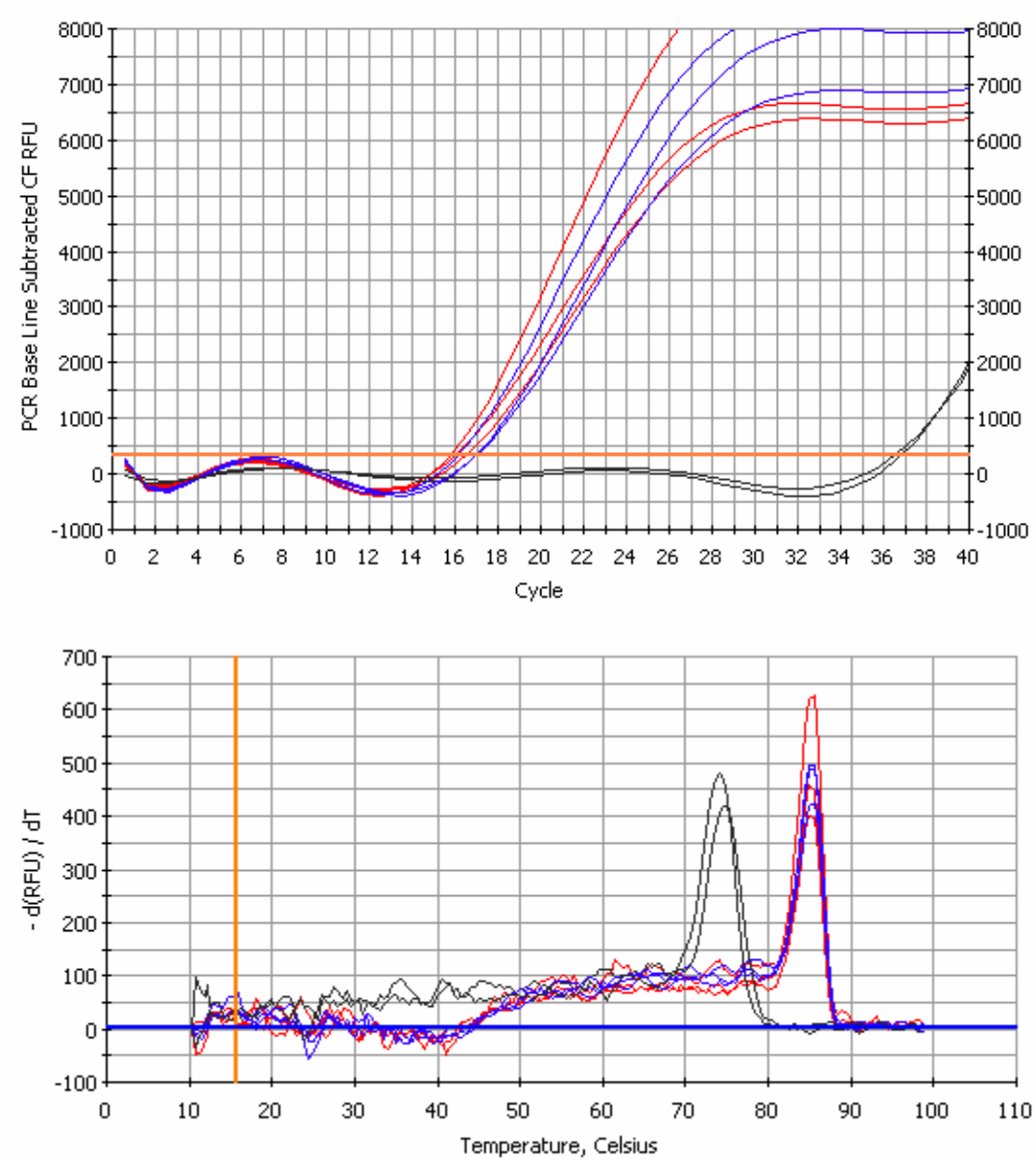

Figure 7 Real-time PCR reactions containing RNA from the second exposure of worms exposed to *B. thailandensis* ATCC 700388 and *E. coli* OP50 filtered medium for 24 hours. These reactions were run using *lys-8* primers. The upper graph shows amplification curves and the lower graph shows melt curves.
(—) *B. thailandensis* exposed
(—) *E. coli* exposed
(—) No reverse transcriptase control

Table 7 PCR threshold cycles for 2 replications of reactions run using RNA from worms exposed to *B. thailandensis* conditioned medium for 24 hours.

Threshold cycles for first reaction with *lys-8* primers:

Sample	Threshold cycle	Sample	Threshold cycle
B. thailandensis exposed	16.7	*E. coli* exposed	17.6
B. thailandensis exposed	16.4	*E. coli* exposed	17.5
B. thailandensis exposed	34	*E. coli* exposed	17
No reverse trans	35.7	No reverse trans	33.6

Threshold cycles for second reaction with *lys-8* primers:

Sample	Threshold cycle	Sample	Threshold cycle
B. thailandensis exposed	15.8	*E. coli* exposed	17.0
B. thailandensis exposed	16.0	*E. coli* exposed	17.0
B. thailandensis exposed	16.5	*E. coli* exposed	16.1
No reverse trans	36.8	No reverse trans	36.6

The average C_T value for the *B. thailandensis* treatments in the second replication is 16.1 and the average value for the *E. coli* treatments is 16.7, corresponding to a 51% mRNA copy number increase in *B. thailandensis* conditioned worms (P=0.18). The no reverse transcriptase reactions amplify far later than the experimental reactions. The melt curve (Figure 7) shows two peaks near 75 °C corresponding to the no reverse transcriptase controls, and all other reactions show a single peak at ~85 °C.

Expression levels of *nlp-29*.

A representative graph showing reactions run using *nlp-29* primers against RNA from conditioned medium exposures is shown in Figure 8. The data for all replications of this exposure are shown in Table 8, and all reactions were run in triplicate. The average C_T value for the first replication *B. thailandensis* treatments is 19.2 and the average for the first replication *E. coli* treatments is 19.2, representing no difference in concentration between these two samples. The no reverse transcriptase controls amplify much later than the experimental reactions. The melt curve (data not shown) showed two peaks in the 73 °C to 75 °C range for the no reverse transcriptase controls, and the experimental reactions all show what appears to be a major and a minor peak with the major peak at ~74 °C and the minor peak at ~76 °C indicating two products in these reactions.

The average C_T value for the second replication of *B. thailandensis* treatments is 19.0 and the average for the *E. coli* treatments is 19.2, corresponding to a 15% mRNA copy number increase in *B. thailandensis* conditioned worms (P=0.45). The no reverse

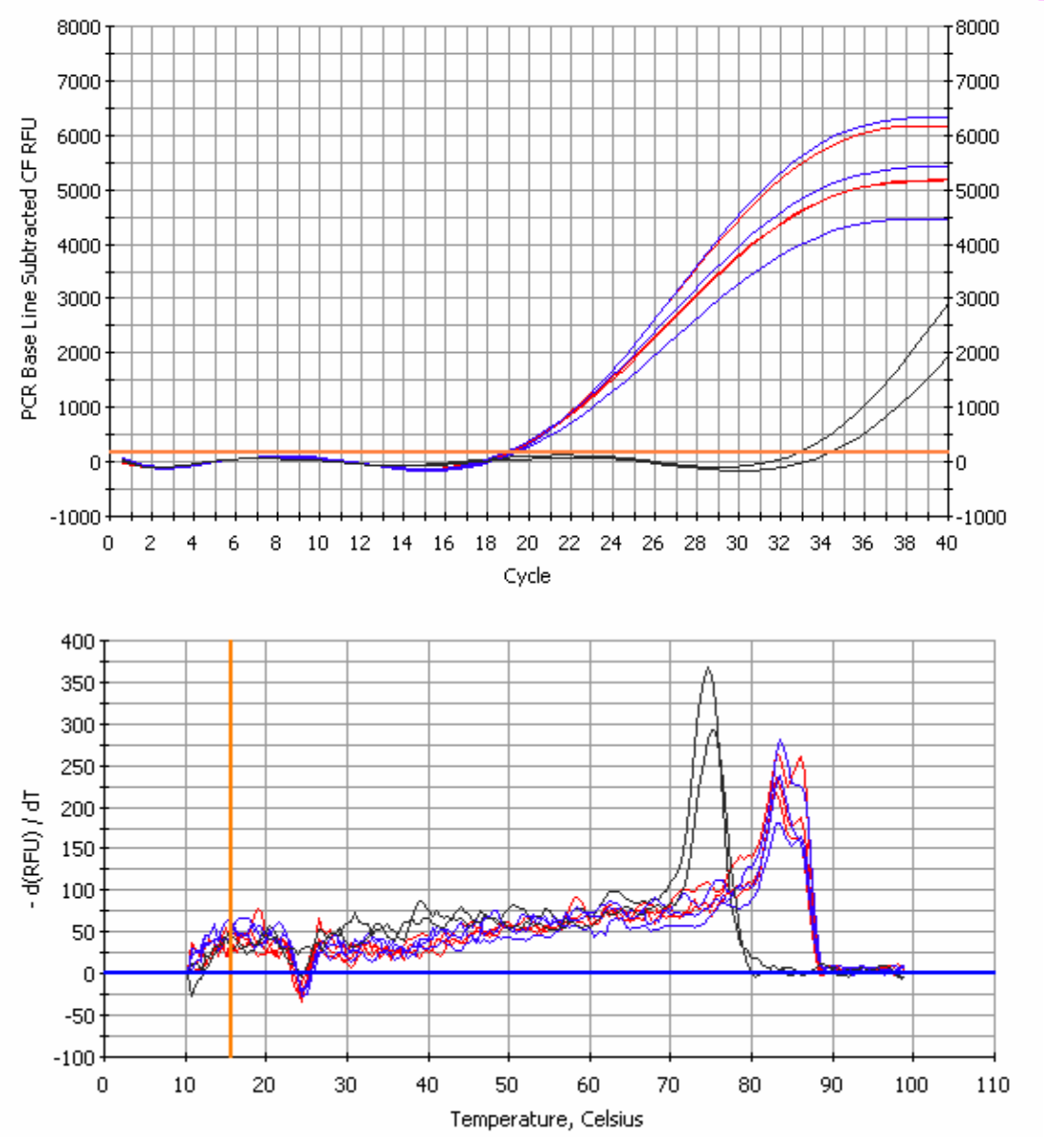

Figure 8 Real-time PCR reactions containing RNA from the second replication of worms exposed to *B. thailandensis* ATCC 700388 and *E. coli* OP50 filtered medium for 24 hours. These reactions were run using *nlp-29* primers. The upper graph shows amplification curves and the lower graph shows melt curves.
(—) *B. thailandensis* exposed
(—) *E. coli* exposed
(—) No reverse transcriptase control

Table 8 PCR threshold cycles for 2 replications of reactions run RNA from worms exposed to *B. thailandensis* conditioned medium for 24 hours. All reactions were run in triplicate.

Threshold cycles for first reaction with *nlp-29* primers:

Sample	Threshold cycle	Sample	Threshold cycle
B. thailandensis exposed	18.8	*E. coli* exposed	19.4
B. thailandensis exposed	19.5	*E. coli* exposed	19.0
B. thailandensis exposed	19.3	*E. coli* exposed	19.2
No reverse trans	33.1	No reverse trans	35.5

Threshold cycles for second reaction with *nlp-29* primers:

Sample	Threshold cycle	Sample	Threshold cycle
B. thailandensis exposed	19.0	*E. coli* exposed	18.9
B. thailandensis exposed	18.9	*E. coli* exposed	19.3
B. thailandensis exposed	19.2	*E. coli* exposed	19.3
No reverse trans	32.8	No reverse trans	34.4

transcriptase controls amplified much later than the experimental reactions, and The melt curve (Figure 8) shows two peaks in the no reverse transcriptase controls around the 75 °C range. Again, there are two peaks in all the experimental reactions at ~74 °C and ~76 °C indicating two products from these reactions.

Expression levels of *abf-1*.

A representative Figure for reactions run using *abf-1* primers against RNA from conditioned medium exposures is shown in Figure 9. The data for all replications of these reactions is shown in Table 9, and all reactions were run in triplicate. The average C_T value for both the *B. thailandensis* and the *E. coli* treatments in the first replication is 19.2, indicating no difference in copy number between these two samples. The no reverse transcriptase controls amplified much later than the experimental reactions. The melt curve (data not shown) had three peaks collectively for the no reverse transcriptase controls with one reaction having one peak and the other reaction having 3, indicating multiple products. The experimental reactions show at least two peaks at ~76 °C and ~83 °C, with some reactions varying from this slightly. This indicates at least three products from these reactions.

The average C_T value for the second replication of *B. thailandensis* treatments is 20.3 and that for the *E. coli* treatments is 21.5, corresponding to a 2.30 fold mRNA copy number increase in *B. thailandensis* conditioned worms (P=0.010). The no reverse transcriptase controls amplified much later than the experimental reactions. The melt curve (data not shown) showed one identical peak at ~83 °C and one separate peak (at

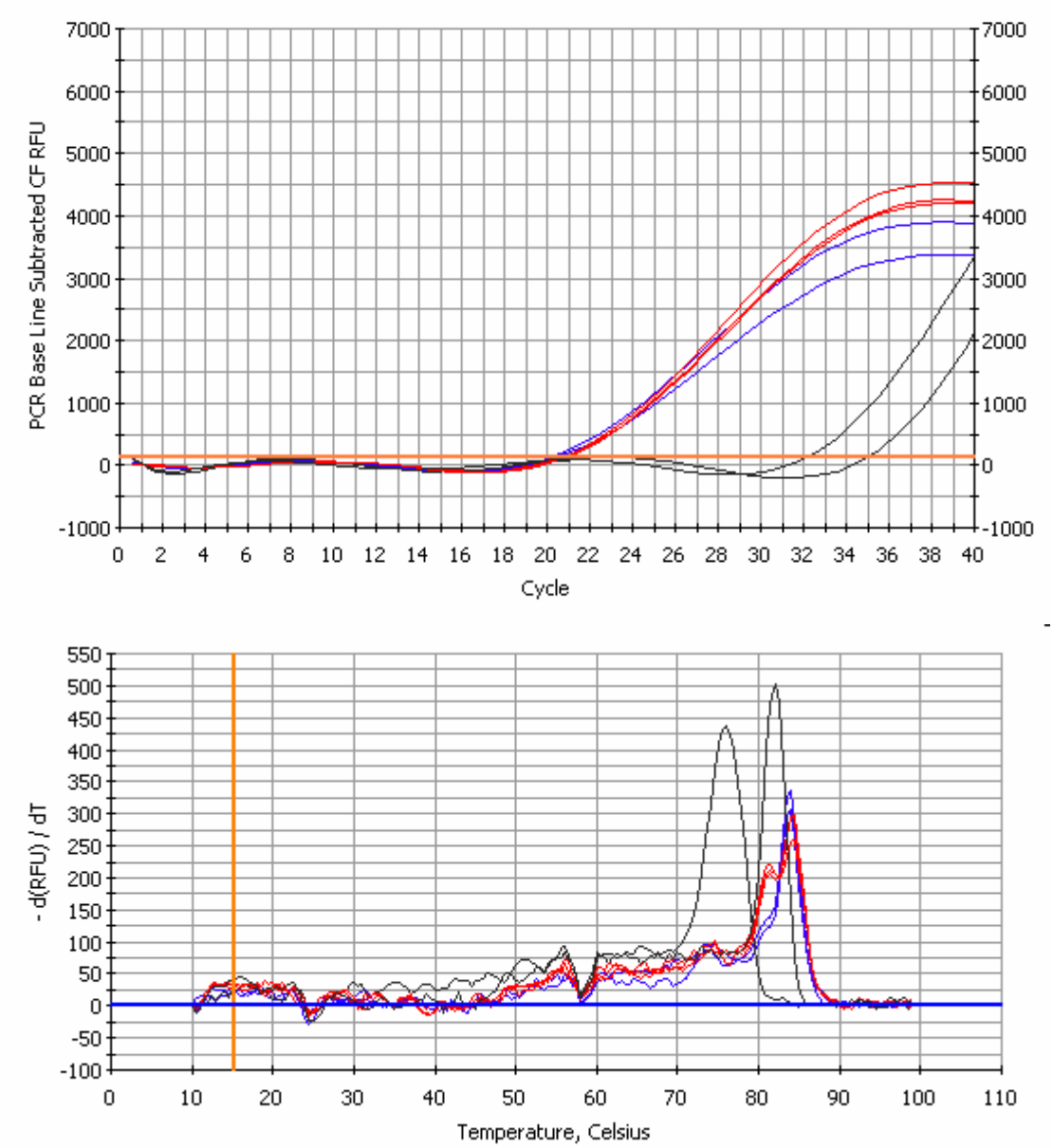

Figure 9 Real-time PCR reactions containing RNA from the third replication of worms exposed to *B. thailandensis* ATCC 700388 and *E. coli* OP50 filtered medium for 24 hours. These reactions were run using *abf-1* primers. The upper graph shows amplification curves and the lower graph shows melt curves.
(—) *B. thailandensis* exposed
(—) *E. coli* exposed
(—) No reverse transcriptase control

Table 9 PCR threshold cycles for 3 replications of reactions run using RNA from worms exposed to *B. thailandensis* conditioned medium for 24 hours. All reactions were run in triplicate

Threshold cycles for first reaction with *abf-1* primers:

Sample	Threshold cycle	Sample	Threshold cycle
B. thailandensis exposed	18.8	*E. coli* exposed	19.4
B. thailandensis exposed	19.5	*E. coli* exposed	19.0
B. thailandensis exposed	19.3	*E. coli* exposed	19.2
No reverse trans	33.1	No reverse trans	35.5

Threshold cycles for second reaction with *abf-1* primers:

Sample	Threshold cycle	Sample	Threshold cycle
B. thailandensis exposed	20.3	*E. coli* exposed	22.0
B. thailandensis exposed	20.3	*E. coli* exposed	21.5
B. thailandensis exposed	20.4	*E. coli* exposed	21.1
No reverse trans	33.4	No reverse trans	32.7

Threshold cycles for third reaction with *abf-1* primers:

Sample	Threshold cycle	Sample	Threshold cycle
B. thailandensis exposed	20.8	*E. coli* exposed	20.3
B. thailandensis exposed	20.9	*E. coli* exposed	20.4
B. thailandensis exposed	20.8	*E. coli* exposed	N/A
No reverse trans	32.1	No reverse trans	34.9

.

~75 °C and 75 °C) for the no reverse transcriptase controls. The experimental reactions showed two peaks at ~83 °C and ~85 °C.

The average C_T value for the third replication of *B. thailandensis* treatments is 20.8 and that for the *E. coli* treatments is 20.4, corresponding to a 32% mRNA copy number decrease in *B. thailandensis* conditioned worms (P=0.0034). One of the replications of the *E. coli* treatments was dropped prior to beginning the run. The two no reverse transcriptase reactions show single but separate peaks at ~75 °C and ~83 °C indicating a single but different product in each (Figure 9). The experimental reactions show the same two peaks as in the previous replications at ~82 °C and ~84 °C.

Expression levels of *abf-2*.

A representative graph for reactions run with *abf-2* primers against RNA from conditioned medium exposures are shown Figure 10. The data for all replications of these reactions is shown in Table 10, and all reactions were run in triplicate. The average C_T value for the first replication of the *B. thailandensis* treatments is 20.4 and that for the *E. coli* treatments is 18.6, corresponding to a 3.48 fold mRNA copy number decrease in *B. thailandensis* conditioned worms (P=0.017). The no reverse transcriptase controls amplify much later than the experimental reactions. The melt curve (data not shown) showed one peak each for the no reverse transcriptase controls in the 76 °C range. The experimental reactions all showed a single peak at ~86 °C.

The average C_T value for the second replication of *B. thailandensis* treatments is 19.8 and that for the *E. coli* treatments is 19.2, corresponding to a 52% mRNA copy

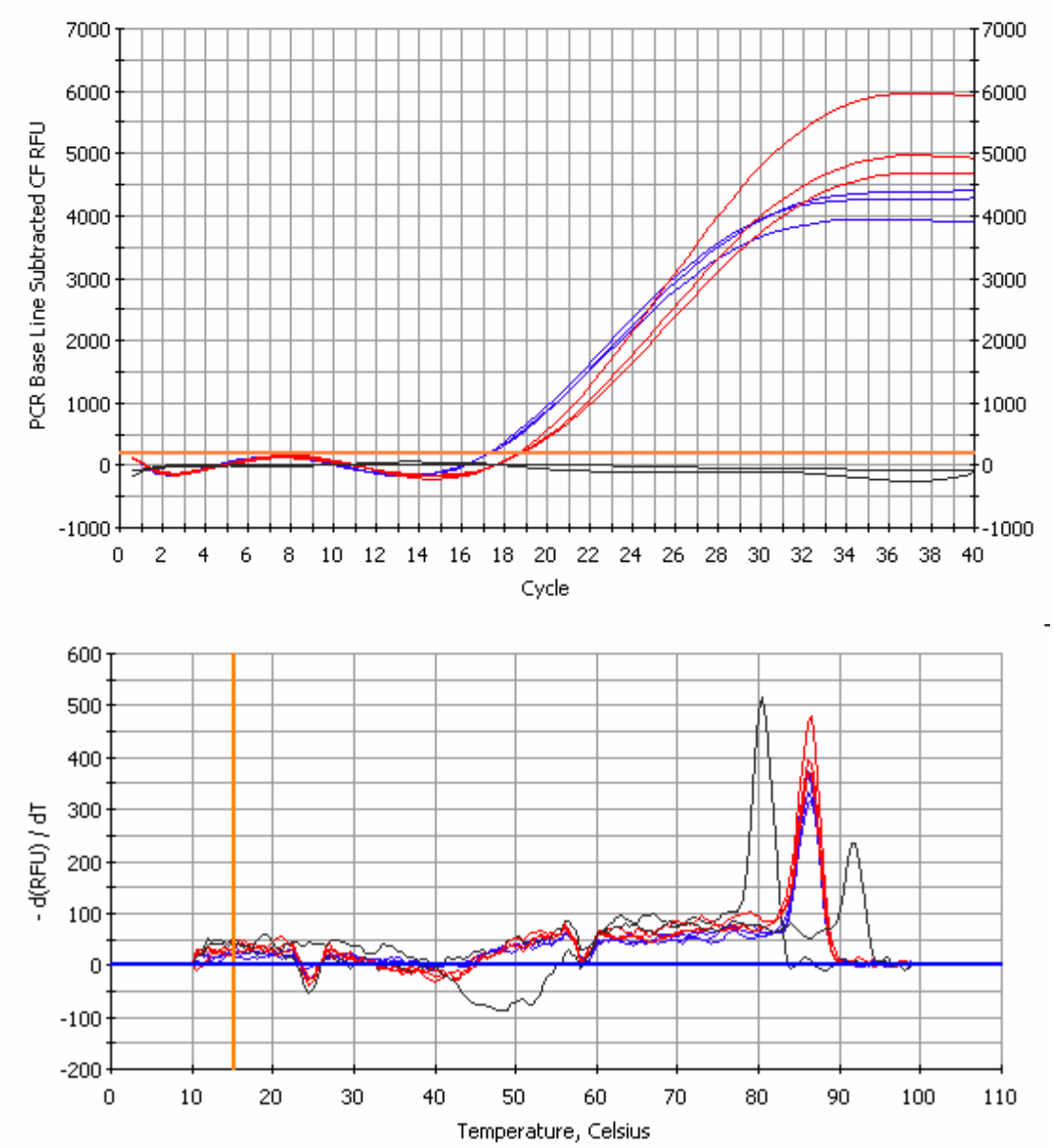

Figure 10 Real-time PCR reactions containing RNA from the third replication of worms exposed to *B. thailandensis* ATCC 700388 and *E. coli* OP50 filtered medium for 24 hours. These reactions were run using *abf-2* primers. The upper graph shows amplification curves and the lower graph shows melt curves.
(—) *B. thailandensis* exposed
(—) *E. coli* exposed
(—) No reverse transcriptase control

Table 10 PCR threshold values for 3 replications of reactions run using RNA from worms exposed to *B. thailandensis* conditioned medium for 24 hours. Each reaction was run in triplicate.

Threshold cycles for first reaction with *abf-2* primers:

Sample	Threshold cycle	Sample	Threshold cycle
B. thailandensis exposed	20.0	*E. coli* exposed	19.3
B. thailandensis exposed	20.4	*E. coli* exposed	18.6
B. thailandensis exposed	20.9	*E. coli* exposed	18.0
No reverse trans	46.2	No reverse trans	38.0

Threshold cycles for second reaction with *abf-2* primers:

Sample	Threshold cycle	Sample	Threshold cycle
B. thailandensis exposed	42.9	*E. coli* exposed	19.3
B. thailandensis exposed	19.8	*E. coli* exposed	19.5
B. thailandensis exposed	19.9	*E. coli* exposed	18.7
No reverse trans	37.3	No reverse trans	47.9

Threshold cycles for third reaction with *abf-2* primers:

Sample	Threshold cycle	Sample	Threshold cycle
B. thailandensis exposed	18.7	*E. coli* exposed	17.3
B. thailandensis exposed	18.9	*E. coli* exposed	17.4
B. thailandensis exposed	18.8	*E. coli* exposed	17.2
No reverse trans	45.6	No reverse trans	41.6

number decrease in *B. thailandensis* conditioned worms (P=0.12). One of the *B. thailandensis* experimental reactions was left out of these calculations due to its failure to amplify. The no reverse transcriptase controls amplify much later than the experimental reactions. The melt curve (data not shown) showed two peaks in one no reverse transcriptase control (at ~81 °C and ~86 °C) and single peak in the other at ~80 °C. The experimental reactions (aside from the excluded *B. thailandensis* reaction) all showed a single peak at ~86 °C.

The average C_T value for the third replication of *B. thailandensis* treatments is 18.8 and that for the *E. coli* treatments is 17.3, corresponding to a 2.83 fold mRNA copy number decrease in *B. thailandensis* conditioned worms ($P=5.16x10^{-5}$). The no reverse transcriptase controls amplify much later than the experimental reactions. The melt curve (Figure 10) showed single but separate peaks in the two no reverse transcriptase controls (at ~80 °C and ~92 °C) and a single peak for all experimental reactions at ~86 °C.

Timed reactions.

The reactions run using *lys-1* and *abf-2* primers against RNA from worms exposed to *B. thailandensis* or *E. coli* in rich medium for 3 hours are shown in Figures 11 and 12. These data are also shown in Table 11, and all reactions were run in triplicate. The amplification data for the *lys-1* reactions from this exposure are shown in Figure 11 and Table 11. The average C_T value for the *B. thailandensis* treatment is 16.7 and the average for the *E. coli* treatment is 18.7, corresponding to a 2.63 fold

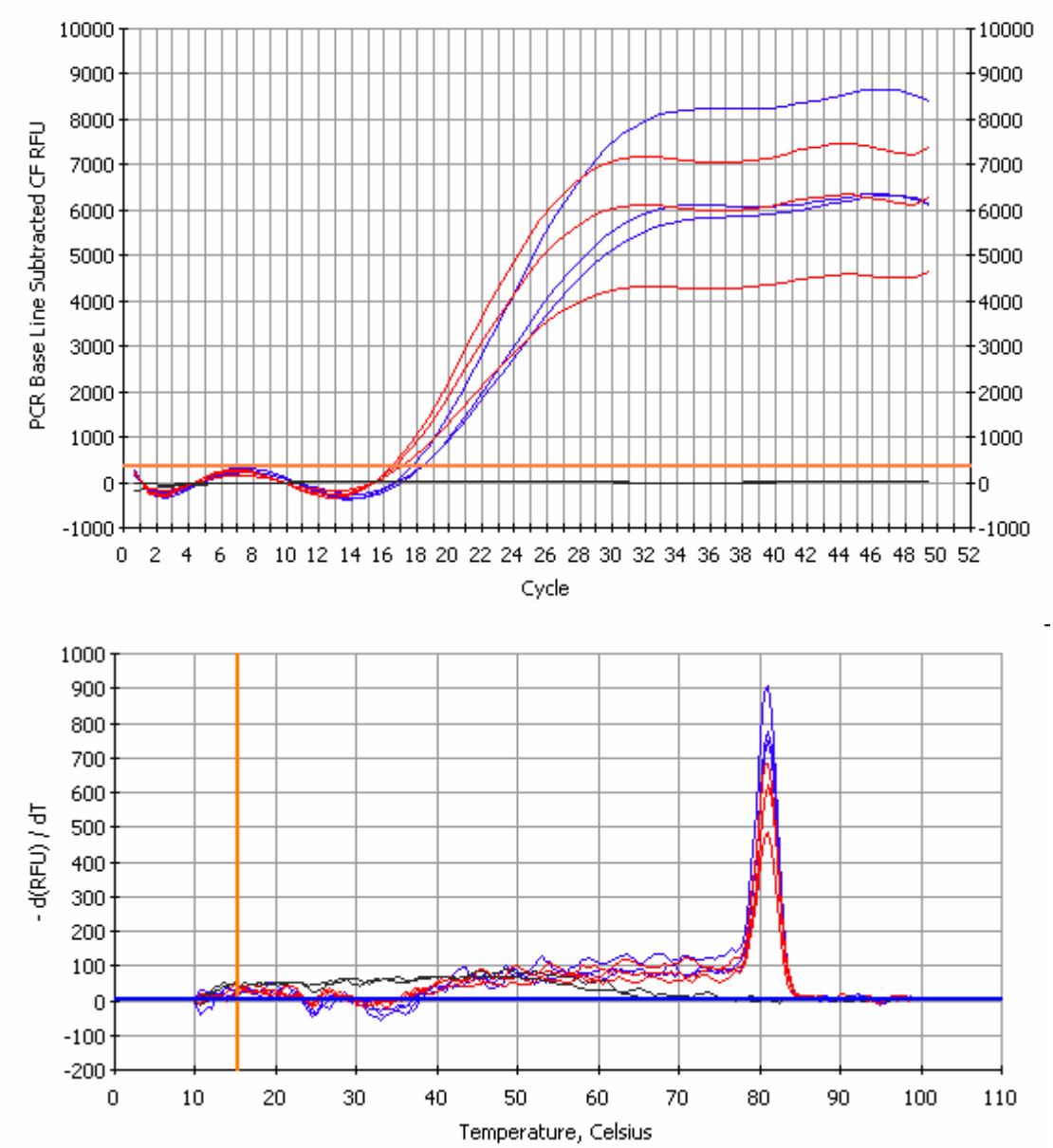

Figure 11 Real-time PCR reactions containing RNA from worms exposed to *B. thailandensis* ATCC 700388 and *E. coli* OP50 in rich medium for 3 hours. These reactions were run using *lys-1* primers. The upper graph shows amplification curves and the lower graph shows melt curves.
(—) *B. thailandensis* exposed
(—) *E. coli* exposed
(—) No reverse transcriptase control

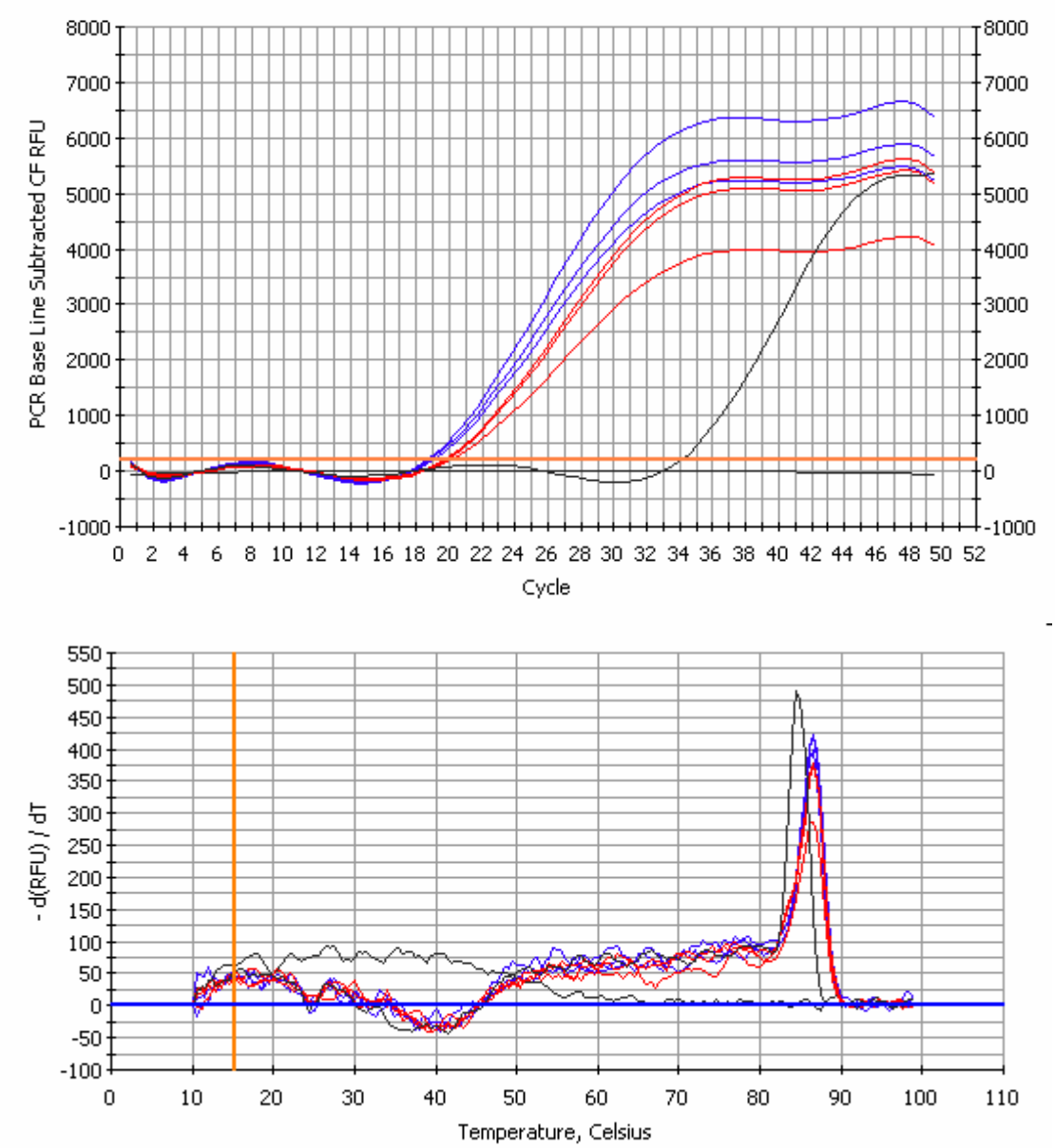

Figure 12 Real-time PCR reactions containing RNA from worms exposed to *B. thailandensis* ATCC 700388 and *E. coli* OP50 in rich medium for 3 hours. These reactions were run using *abf-2* primers. The upper graph shows amplification curves and the lower graph shows melt curves.
(—) *B. thailandensis* exposed
(—) *E. coli* exposed
(—) No reverse transcriptase control

Table 11 PCR threshold values for reactions run using RNA from worms exposed to *B. thailandensis* in rich medium for 3 hours. Each reaction was run in triplicate

Threshold cycles for reactions against *1ys-1* (Figure 11):

Sample	Threshold cycle	Sample	Threshold cycle
B. thailandensis exposed	16.5	*E. coli* exposed	17.7
B. thailandensis exposed	17.0	*E. coli* exposed	18.3
B. thailandensis exposed	16.6	*E. coli* exposed	18.3
No reverse trans	N/A	No reverse trans	N/A

Threshold cycles for reactions against *abf-2* (Figure 12):

Sample	Threshold cycle	Sample	Threshold cycle
B. thailandensis exposed	19.8	*E. coli* exposed	19.0
B. thailandensis exposed	19.7	*E. coli* exposed	18.7
B. thailandensis exposed	20.0	*E. coli* exposed	18.8
No reverse trans	34.0	No reverse trans	N/A

.

mRNA copy number increase in *B. thailandensis* exposed worms (P=0.0051). The no reverse transcriptase controls did not amplify, and the melt curve (Figure 11) shows a single peak at ~82 °C for all experimental reactions.

The amplification data for the *abf-2* reactions from this exposure is shown in Figure 12 and Table 11. The average C_T value for the *B. thailandensis* treatment is 19.8 and the average for the *E. coli* treatment is 18.8, corresponding to a 2 fold mRNA copy number decrease in the *B. thailandensis* exposures (P=0.0013). The no reverse transcriptase control run on the *B. thailandensis* treatment RNA sample amplifies much later than the experimental reactions run with this sample. The other no reverse transcriptase control does not amplify. The melt curve (Figure 12) shows one peak for the no reverse transcriptase control that amplified at ~85 °C. Again, the experimental reactions show a single peak at ~86 °C.

High Statistical Stringency Real-Time PCR

The results of RTPCR run for highly stringent analysis are shown in Figures 13 through 15, and in Table 12. In a non-stringent analysis of the results, the reference gene (*rla-1*) has an average threshold cycle in *E. coli* exposures of 14.82, and in *B. thailandensis* exposures of 14.60, which corresponds to a 16% increase in mRNA copy number in the *B. thailandensis* exposed worms (P=0.39). For *abf-2*, this analysis shows an average threshold cycle of 18.42 for *E. coli* exposed worm and 18.05 for *B. thailandensis* exposed worms, corresponding to a 29% increase in mRNA copy

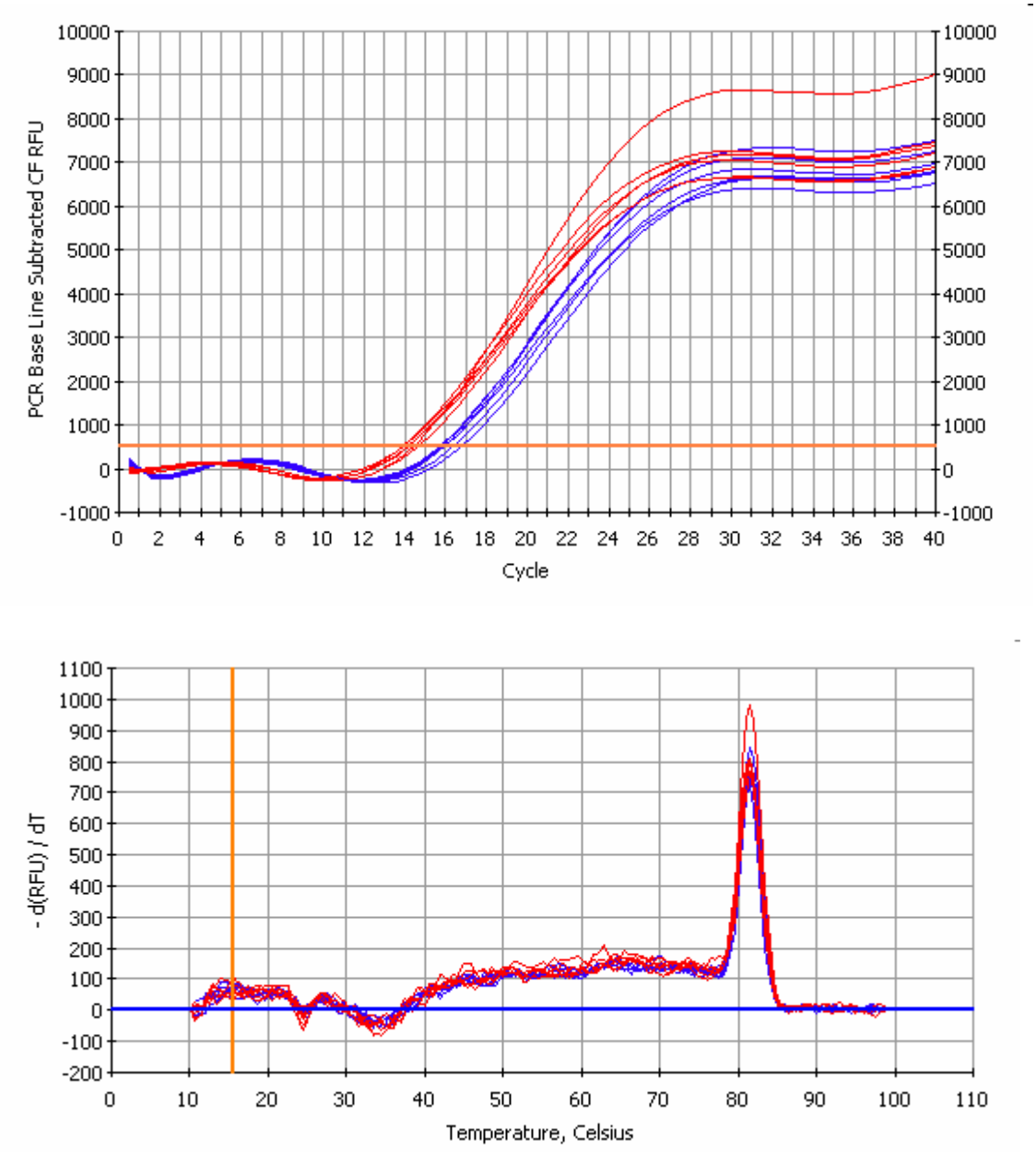

Figure 13 Amplification and melt curve graphs for reactions run using *lys-1* primers against RNA from worms exposed to *E. coli* and *B. thailandensis* in M9. The upper graph shows amplification curves and the lower graph shows melt curves.
(—) *B. thailandensis* exposed
(—) *E. coli* exposed

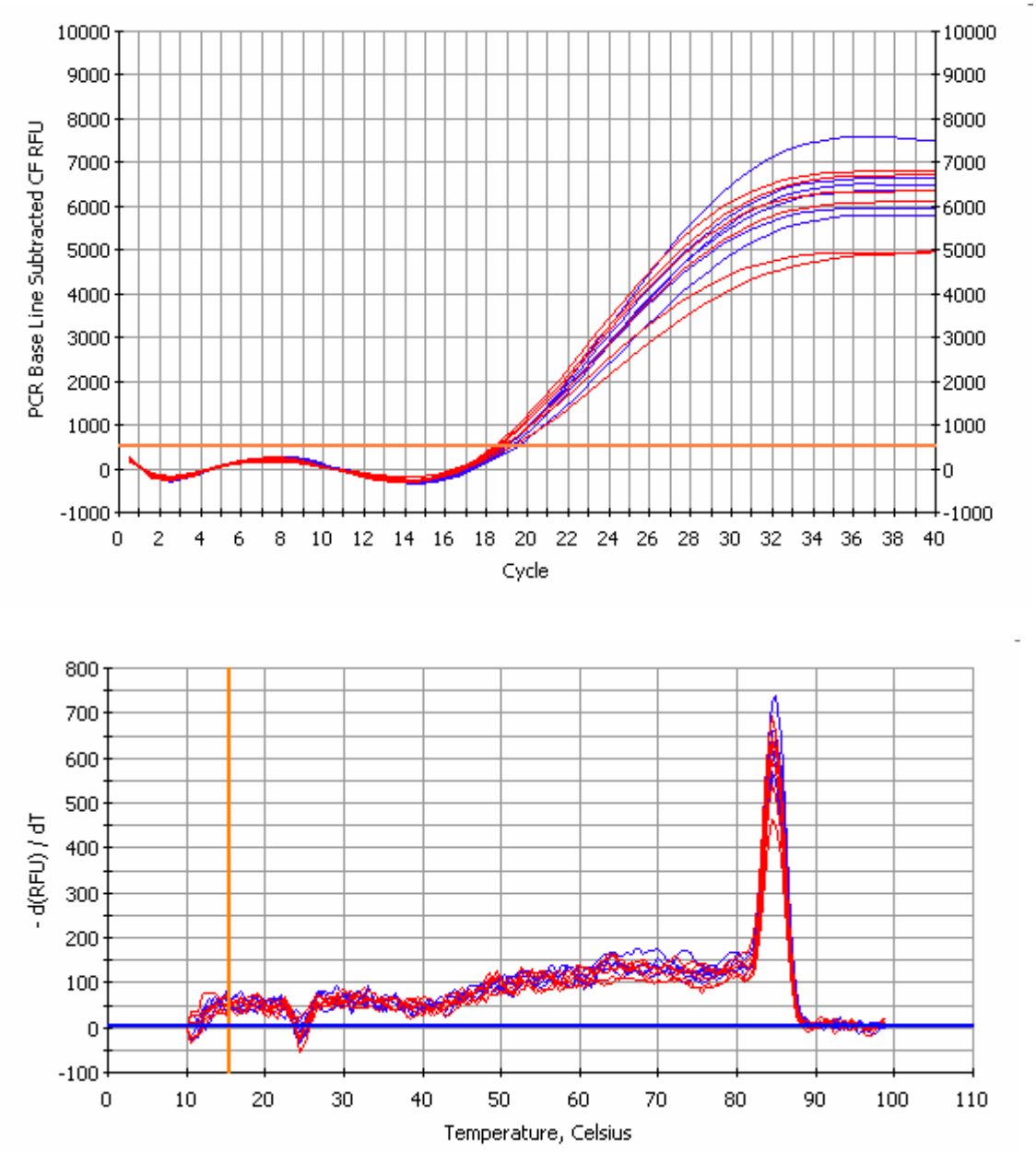

Figure 14 Amplification and melt curve graphs for reactions run using *abf-2* primers against RNA from worms exposed to *E. coli* and *B. thailandensis* in M9. The upper graph shows amplification curves and the lower graph shows melt curves.
(—) *B. thailandensis* exposed
(—) *E. coli* exposed

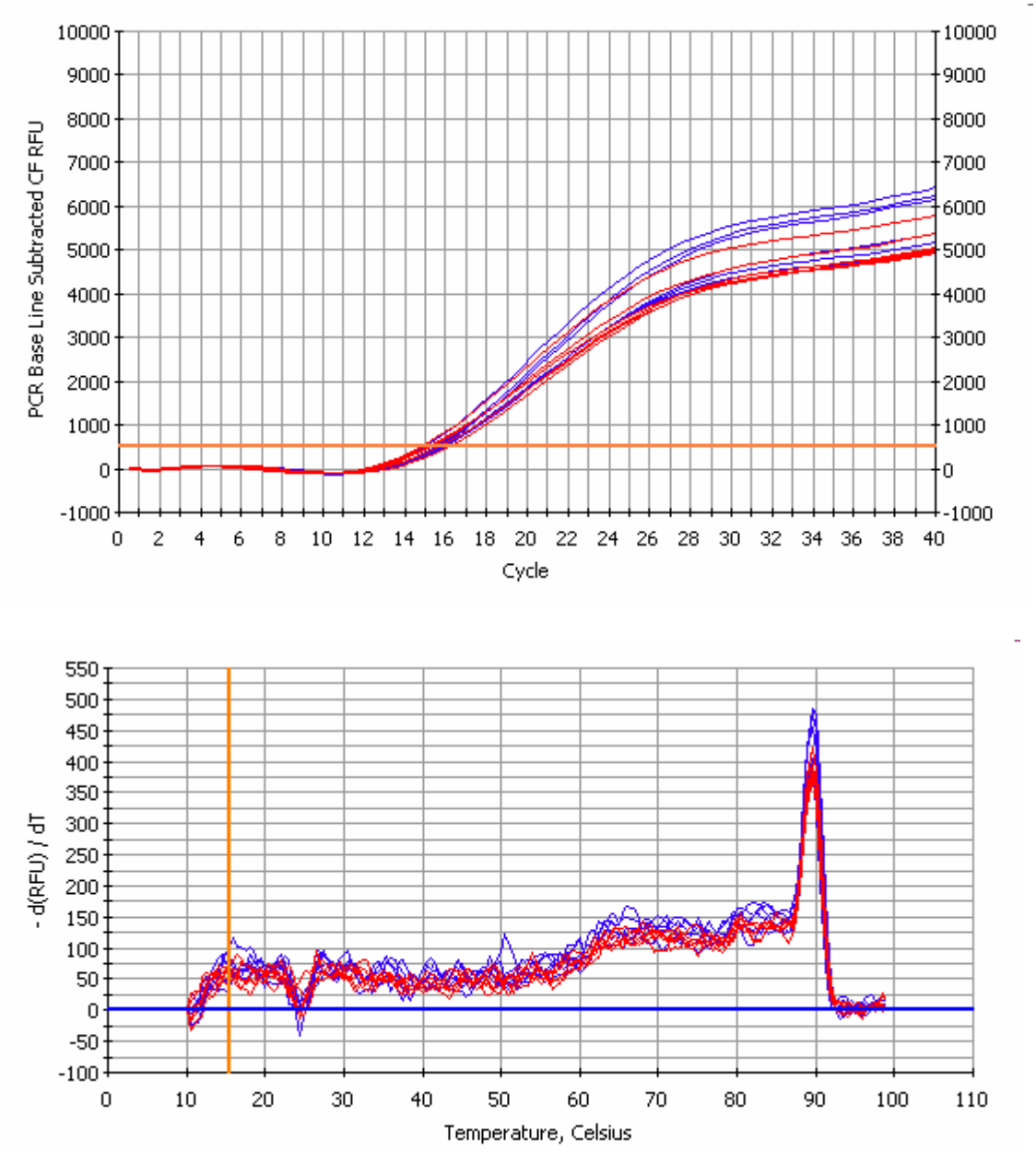

Figure 15 Amplification and melt curve graphs for reactions run using *rla-1* primers against RNA from worms exposed to *E. coli* and *B. thailandensis* in M9. The upper graph shows amplification curves and the lower graph shows melt curves.
(—) *B. thailandensis* exposed
(—) *E. coli* exposed

Table 12 Threshold cycle values for reactions run in high stringency method. Six biological replicates were run of infections and controls. Each RNA isolate from each infection and control was run against three primer sets: *rla-1, lys-1* and *abf-2.*

Exposure	Gene	Threshold cycle	Exposure	Gene	Threshold cycle
E. coli	*rla-1*	15.1	*B. thailandensis*	*rla-1*	14.8
E. coli	*rla-1*	14.9	*B. thailandensis*	*rla-1*	14
E. coli	*rla-1*	14.9	*B. thailandensis*	*rla-1*	14.9
E. coli	*rla-1*	14.2	*B. thailandensis*	*rla-1*	14.4
E. coli	*rla-1*	15.1	*B. thailandensis*	*rla-1*	14.2
E. coli	*rla-1*	14.7	*B. thailandensis*	*rla-1*	15.3
E. coli	*abf-2*	18.3	*B. thailandensis*	*abf-2*	18
E. coli	*abf-2*	18.8	*B. thailandensis*	*abf-2*	18.5
E. coli	*abf-2*	18.1	*B. thailandensis*	*abf-2*	18
E. coli	*abf-2*	18.3	*B. thailandensis*	*abf-2*	17.8
E. coli	*abf-2*	18.4	*B. thailandensis*	*abf-2*	18.2
E. coli	*abf-2*	18.6	*B. thailandensis*	*abf-2*	17.8
E. coli	*lys-1*	15.3	*B. thailandensis*	*lys-1*	13.9
E. coli	*lys-1*	16.2	*B. thailandensis*	*lys-1*	13.6
E. coli	*lys-1*	15.2	*B. thailandensis*	*lys-1*	14.1
E. coli	*lys-1*	15.5	*B. thailandensis*	*lys-1*	13.2
E. coli	*lys-1*	15.8	*B. thailandensis*	*lys-1*	13.3

number for *B. thailandensis* exposed worms (P=0.03). For *lys-1*, this analysis showed the average threshold cycle for *E. coli* exposed worms as 15.53, and that for *B. thailandensis* exposed worms as 13.62, corresponding to a 3.78 fold increase in mRNA copy number in *B. thailandensis* exposed worms ($P=4.43x10^{-6}$). All three primer sets produced a single unique peak in the melt curve analysis.

In a highly stringent analysis, the rla-1 expression data are used as a reference to quantify the level of experimental noise (that is, difference unrelated to the changed experimental variable of interest) between conditions. In this analysis, there is no significant change in abf-2 expression between infected and uninfected conditions. With respect to lys-1, there is a 2.12 fold increase in mRNA copy number in B. thailandensis exposed worms, with the lower expression level increase in the 95% confidence interval being 26% and the upper expression level increase in this interval being 3.55 fold. In other words, in a highly stringent statistical analysis of these results, lys-1 expression is increased in worms exposed to B. thailandensis between 26% and 3.55 fold with 95% confidence when compared to worms exposed to E. coli.

Bioinformatics

The CSαβ-type (defensin-like) peptides analyzed here all had multiple properties in common (Table 13 and Figure 16). All the sequences for known defensin-like peptides were less than 200 amino acids in length; all had numerous Cysteine residues; most had basic predicted PI; all but two had predicted transmembrane segments near the amino-terminal end of the sequence; all but one had a hydropathy profile that included a

strongly hydrophobic N-terminal region followed by a precipitous drop in hydrophobicity; and, most had numerous significant NCBI protein blast hits.

These features, together, did not prove to be common in sequences of under 200 amino acids harvested from human chromosome 2 (see materials and methods). Representative examples of the 130 screened are shown in Figure 17 and 18 and in Table 14. In particular, the distinctive hydropathy profile and predicted transmembrane sequences were rare, indicating that these may be good characters to use when data mining for defensin-like sequences. Figure 17 has six examples of non-characteristic hydropathy profiles. Of the 130 sequences screened, only three clearly had the distinctive hydropathy profile of the defensin-like peptides, and only three had predicted transmembrane segments in the N-terminal region (Table 14). Of those peptides, two have both features: Gnomon predicted sequences hmm132143 and hmm120686. Both of these sequences are short, have basic predicted PIs, have the appropriate transmembrane segments, have characteristic hydropathy and multiple significant cross species protein blast hits. In addition to these characters, both have predicted secretion signals (Bendtsen et al. 2004) and one, hmm132143, has an associated cleavage site (data not shown).

Hmm132143 is also listed as a reference sequence in the NCBI database (accession number XM 374010) and is not listed as having any known function. A CLUSTALW alignment of this sequence to several other defensins shows significant identity (Figure 19 and Figure 21). Gnomon predicted sequence hmm 120686 also shows significant sequence identity to known human defensins (Figure 20).

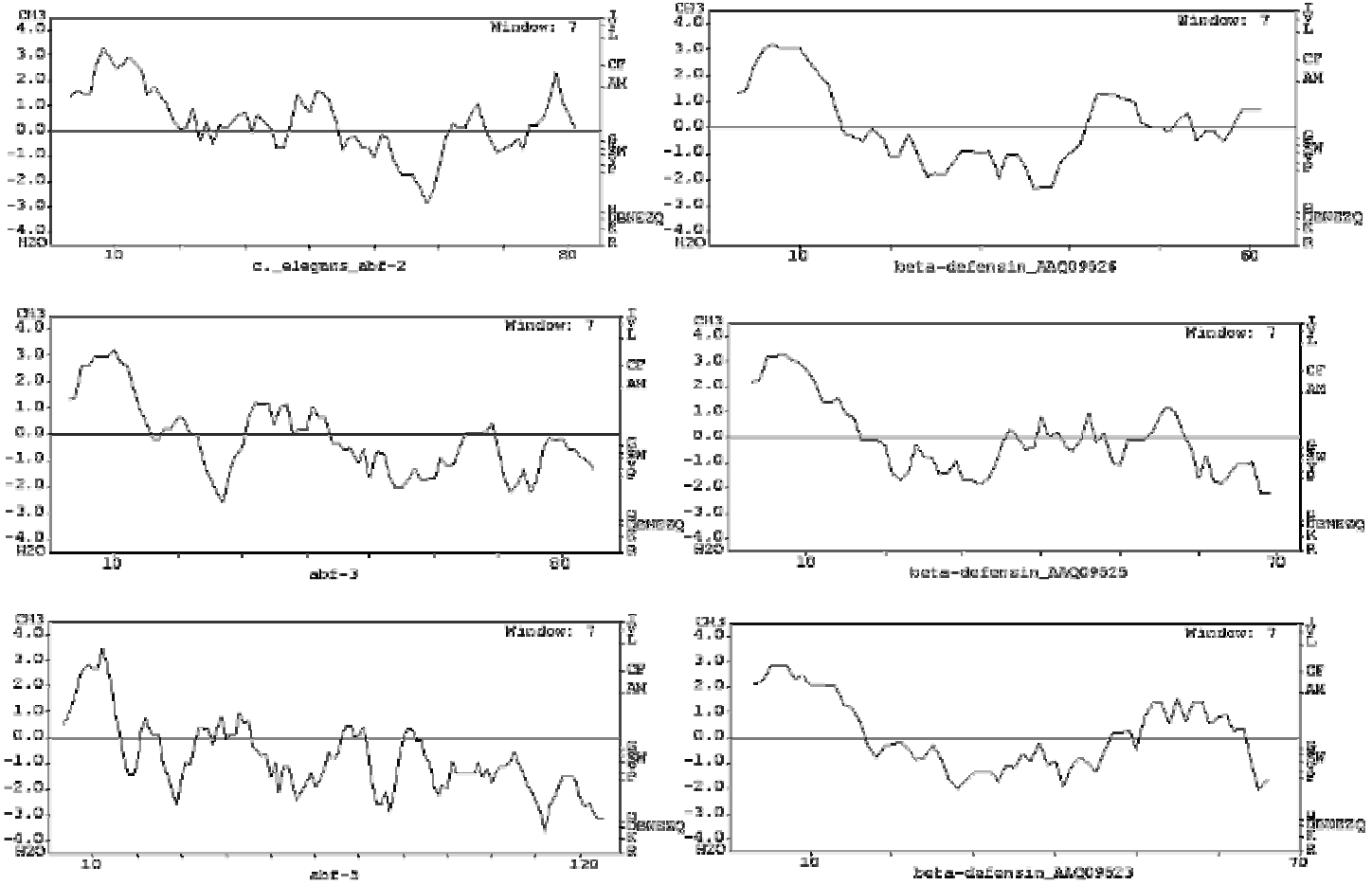

Figure 16 Hydropathy plots for six selected defensin and defensin-like peptides all showing a stereotypical pattern of 10 to 20 hydrophobic amino acids at the amino-terminal end of the peptide sequence followed by a general, and relatively rapid, decrease in hydrophobicity moving toward the carboxy-terminal. In some instances there is also an increase in hydrophobicity near the carboxy-terminal end.

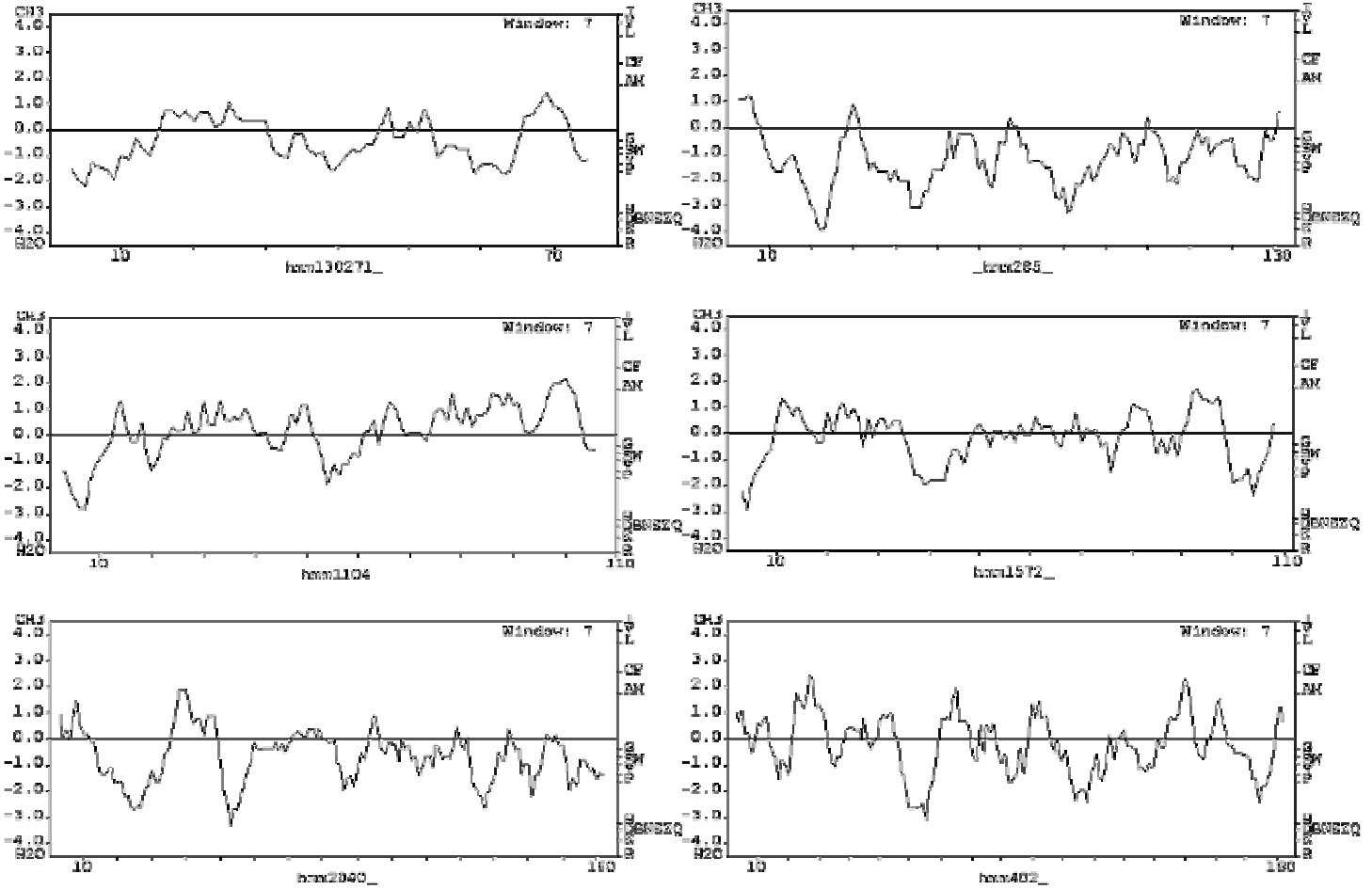

Figure 17 Six selected examples of hydropathy plots *not* showing a stereotypical defensin-like pattern. Non-stereotypical patterns are present in the large majority of short predicted peptide sequences examined in this study. There is no trend in these plots resembling the trend observed in defensin-like peptides (Figure 21).

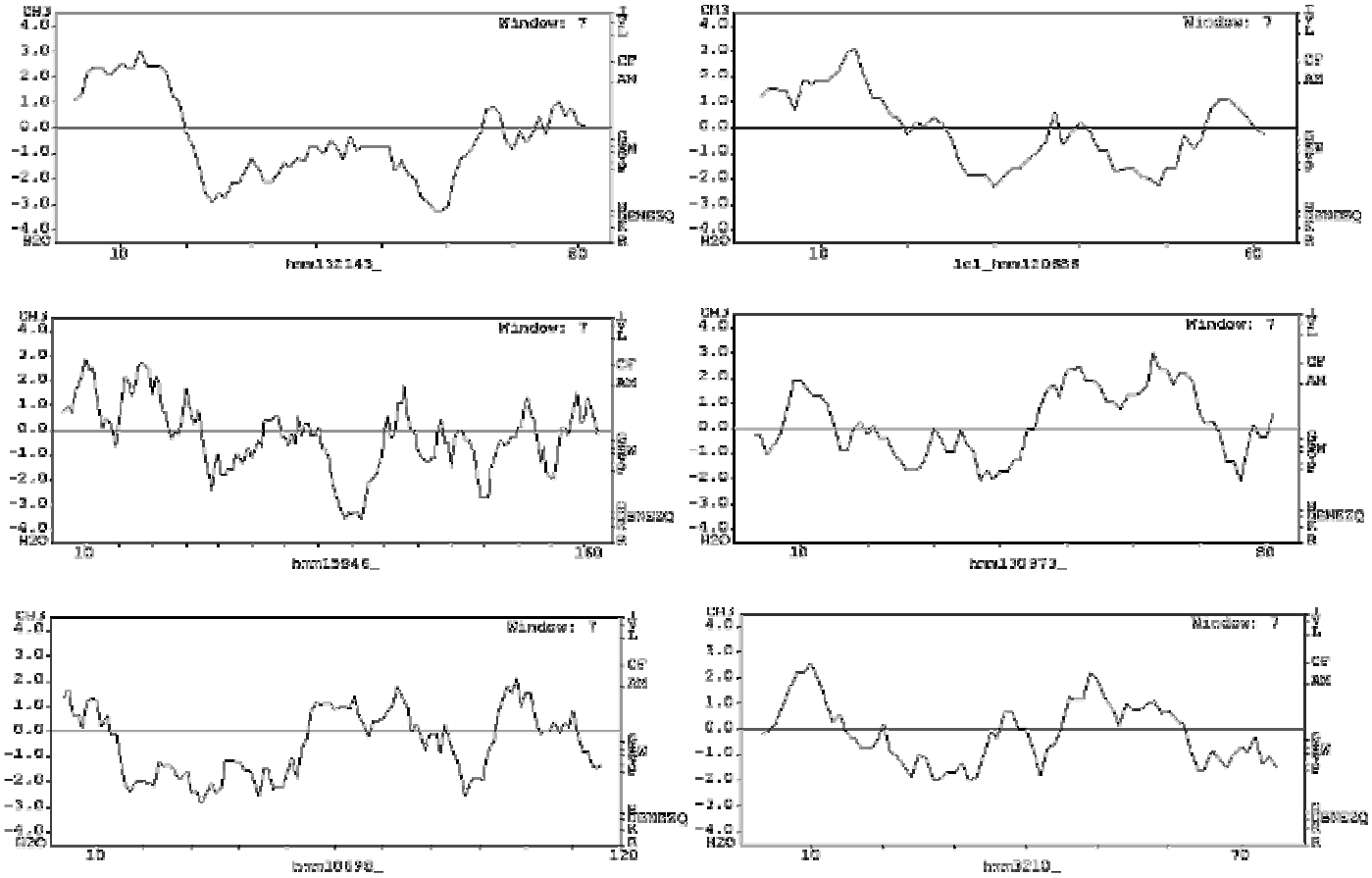

Figure 18 Hydropathy plots of hypothetical peptide sequences identified as having antimicrobial-like features. These plots correspond to those hypothetical sequences marked with an asterisk in Table 13. The two upper plots show strong similarity to the plots of defensin-like peptides. Specifically, hydrophobic amino-terminal ends followed by a relatively rapid decrease in hydrophobicity toward the carboxy-terminal end of the sequence. The bottom two plots, and the middle right plot, show a more pronounce hydrophobic region toward the carboxy-terminal end of the sequence.

```
Consensus key (see documentation for details)
* - single, fully conserved residue
: - conservation of strong groups
. - conservation of weak groups
  - no consensus


CLUSTAL W (1.81) multiple sequence alignment


hmm132143                MRPLLCALAGLALLCAVGALADGREDRGSPGDTGERPAGPARGPGLEPAR
beta-defensin_AAQ09525   MR--IAVLL-FAIFFFMSQVLPAR---GKFKEICERPNGSCRDFCLETEI
                         **  :..*  :*::  :. :  .*   *.  :  *** *..*.  **.

hmm132143                GTLQPRPRPPRKRWLLSPGAGAQQLEVVHLPGSTL
beta-defensin_AAQ09525   HVGRCLNSQP---CCLPLGH-QPRIEST-TPKKD-
                          . :     *     *. *    ::* .  * .


hmm132143                MRPLLCALAGLALL----------------------CAVG-ALADGRED
beta-defensin_AAQ09524   MKLLLLALPMLVLLPQVIPAYSGEKKCWNRSGHCRKQCKDGEAVKDTCKN
                         *: ** **. *.**                        *  * *: *  ::

hmm132143                RGS---PGDTGER--PAG---PARG--PGLEPARGTLQPRPR----PPRK
beta-defensin_AAQ09524   LRACCIPSNEDHRRVPATSPTPLSDSTPGIIDDILTVRFTTDYFEVSSKK
                           :   *.: ..*  **    *  .  **:     *::  .     ..:*

hmm132143                RWLLSPGAG-AQQLEVVHLPGSTL
beta-defensin_AAQ09524   DMVEESEAGRGTETSLPNVHHSS-
                           : .. ** . : .: ::  *:
```

Figure 19 The output from a CLUSTALW sequence alignment between Gnomon-predicted sequence hmm132143 and human beta-defensins AAQ09542 and AAQ09525 (Genbank accession numbers). A high degree of conservation can be observed in both alignments.

```
Consensus key (see documentation for details)
* - single, fully conserved residue
: - conservation of strong groups
. - conservation of weak groups
  - no consensus


CLUSTAL W (1.81) multiple sequence alignment


lcl_hmm120686              MAGLRLFLASPLFLLIVWEELSLG--CRSARDKCRKVPQPVPVRASEPPP
beta-defensin_AAQ09526     MRTF-LFLFAVLFFLTPAKNAFFDEKCNKLKGTCKNN-CGKNEELIALCQ
                           *  : *** : **:*   ::  :.  *.. :..*::       .

lcl_hmm120686              KFKKELPISYISLDAKD
beta-defensin_AAQ09526     KFLKCCRTIQPCGSIID
                           ** *       . .  *


---


lcl_hmm120686              MAGLRLFLASPLFL---LIVWEELSLGCRSARDKCRKVPQPVPVRASEPP
beta-defensin_AAQ09525     MRIAVLLFAIFFFMSQVLPARGKFKEICERPNGSCRDFCLETEIHVGRCL
                           *    *::*  :*:   * .  ::.  *. ....**..   . ::...

lcl_hmm120686              PKFKKELPISYIS-LDAKD----
beta-defensin_AAQ09525     NSQPCCLPLGHQPRIESTTPKKD
                            .    **:.: . ::::.
```

Figure 20 The output from a CLUSTALW sequence alignment between Gnomon-predicted sequence hmm120686 and human beta-defensins AAQ09545 and AAQ09526 (Genbank accession numbers). A high degree of conservation can be observed in both alignments.

```
Consensus key (see documentation for details)
* - single, fully conserved residue
: - conservation of strong groups
. - conservation of weak groups
  - no consensus


CLUSTAL W (1.81) multiple sequence alignment


human_132143      M--RPLLCALAGLALLCAVGALADGREDRGSPGDTGERPAGPARGP-GLEPA-RGTLQPR
abf-2             MFVRSLFLALL-LATIVAADIDFSTCARMDVP-ILKKAAQGLCITSCSMQNCGTGSCKKR
                  *  *.*: **  ** : *..   .     . *    : . * .  . .:: .  *: : *

human_132143      P-RPPRKRWLLSPGAGAQQLEVVHLPGSTL
abf-2             SGRPTCVCYRCANGGGDIPLGALIKRG---
                  . **.   :  : *.*   * .:   *


---------------------------------------------------------------------------


human_132143      MR-PLLCALAGLALLCAVGALADGR-EDRGSPGDTGERPAGPARGPGLEPARGTLQPRPR
abf-3             MNFSFLFFIFAFLIGLNKGSVCLTRRTDWGQLGAIFTNPVCDVWCRIRQCGPGQCKEDPM
                  *. .:*  : .: :    *::.  *  * *. *    .*.  .     : . *  :  *

human_132143      PPRKRWLLSPGAGAQQLEVVHLPGST-L-
abf-3             TSDEAQCVCEKCYRDSYGNAIYPGNNGLQ
                  .. :   :.  .  :.   .  **.. *
```

Figure 21 The output from a CLUSTAWL sequence alignment between Gnomon predicted sequence hmm132143 and two *C. elegans abf* genes. A high degree of conservation can be observed in both alignments

Table 13 All peptides are defensins with the exception of those labeled ASABF or ABF. For all sequences obtained from NCBI, the accession number is given to the right of the designation. The PI is a prediction based on assumed pKa's of side groups and the amino and carboxy termini; cysteines are also included in the PI calculation. The transmembrane segment prediction shows, by sequence number, the amino acids predicted to be within a transmembrane region. Characteristic hydropathy plots are shown in figure 30.

Designation	Amino A. length	cysteine #	PI	TMS prediction	Distinctive Hydropathy Plot	Significant Protein Blast Hits
Human β-defensin AAQ09526	65	7	8.67	3-31	Yes	57
Human β-defensin AAQ09525	73	6	8.31	3-27	Yes	40
Human β-defensin AAQ09524	123	6	7.08	6-34	Yes	70
Human β-defensin AAQ09523	70	6	7.64	3-27	Yes	28
Human β-defensin AAQ09522	183	6	9.02	None	No	23
Human α-defensin NP_001035965	94	6	6.77	3-28	Yes	177
Hyblaea puera ABQ08056	79	7	6.97	3-25 & 48-66	Yes	100
Triatoma infestans ABD61004	94	7	7.09	4-24	Yes	102
Anopheles quadriannulatus ABB0100	102	8	7.52	4-25	Yes	135
Formica aquilonia AAX20158	95	6	8.58	3-31	Yes	101
Drosophila melanogaster CAA81760	92	7	7.13	3-23	Yes	100
ASABF-alpha BAA11943	93	8	9.74	4-23	Yes	24
ASABF-zeta BAC57992	94	8	10.06	3-31	Yes	21
ASABF-epsilon_BAC41495	65	8	8.09	4-24	Yes	10
ASABF-delta_BAC00499	80	9	8.81	3-31	Yes	25
ASABF-gamma_BAC00498	81	8	8.75	3-31	Yes	24
ASABF-beta_BAC00497	89	8	9.27	3-31	Yes	24
ABF-1	85	9	6.82	None	Yes	19
ABF -2	85	8	9.00	3-31	Yes	23
ABF -3	89	8	6.19	4-23	Yes	11
ABF -4	123	11	7.35	4-23	Yes	12
ABF -5	129	9	4.34	3-31	Yes	12
ABF -6	195	9	8.17	3-23	Yes	4

Table 14 All peptides are predicted by NCBI's Genomon algorithm. The PI is a prediction based on assumed pKa's of side groups and the amino and carboxy termini; cysteines are also included in the PI calculation. The transmembrane segment prediction shows, by sequence number, the amino acids predicted to be within a transmembrane region. Six selected examples of non-characteristic hydropathy are shown in figure 31, and the asterisks designate predicted sequences who's hydropathy plots are shown in figure 32.

Designation	Amino A. length	cysteine #	PI	TMS prediction	Distinctive Hydropathy Plot	Significant Protein Blast Hits
hmm130271	79	1	8.87	None	No	1
hmm130973*	85	5	7.72	49-75	Questionable	1
hmm131441	194	6	10.20	None	No	1
hmm131675	187	11	8.39	None	No	1
hmm131909	149	6	8.56	None	No	3
hmm132143*	85	2	10.93	3-30	Yes	13
hmm132377	20	1	4.65	None	No	20
hmm74228	128	2	10.77	None	Questionable	114
hmm73994	96	1	9.64	None	Questionable	123
hmm285	135	0	11.70	None	No	54
hmm402	186	12	8.46	None	No	144
hmm870	51	3	10.18	None	No	13
hmm1104	110	5	6.30	None	No	20
hmm1572	112	3	8.01	None	No	32
hmm2040	166	4	11.83	None	No	4
hmm120686*	65	2	9.83	6-32	Yes	104
hmm3210*	79	1	10.38	None	Yes	88
hmm8358	129	6	10.38	6-34	No	96
hmm9294	185	6	10.71	153-181	No	282
hmm10698*	120	0	11.29	92-119	Questionable	212
hmm158468*	168	4	9.10	20-43	Questionable	144
hmm22281	195	5	9.40	58-86 & 158-183	No	95
hmm29067	157	14	8.31`	18-42	No	54

DISCUSSION

Gene Expression and Real-Time PCR

There were two very strong reproducible patterns of gene expression that became evident through the course of my experiments when *C. elegans* was exposed to *B. thailandensis*. Namely, the statistically significant upregulation of *lys-1* and the downregulation of *abf-2* in response to *B. thailandensis.* The expression of *lys-1* is important in that it establishes that the worm is, indeed, mounting an immune response against this pathogen, which has not been previously demonstrated. The downregulation of *abf-2* is potentially of great biological significance because of the likely role of this gene in the immune system of the worm, and because there is a secreted product of *B. thailandensis* that appears to be responsible for this downregulation.

To establish the validity of my procedures, I first compared results obtained to those in literature. The expression levels of *lys-1* in response to *S. marcescens* was previously reported to be in the range of 2.3 to 6.1 fold (Mallo et al. 2002). My results show a reproducible induction of this gene in response to *S. marcescens* in the range of 3.5 to 6.1 fold (Table 3). Even though the details of my procedure varied from those used in other studies, consistently reproducible results similar to those reported in the literature were obtained. This, therefore, confirms the validity of my procedures.

Having provided experimental evidence for the validity of my method of gene expression analysis, I turned my experiments to the much less well studied interaction between *B. thailandensis* and *C. elegans.* As discussed in the introduction, two previous

studies (Gan et al. 2002, O'Quinn et al. 2001) have established the pathogenicity of *Burkholderia* sp. These papers focus on the interaction of the bacterium with the worm and the nature of infective death. Both papers describe the existence of a toxin that kills the worm. However, they disagree as to whether the toxin is an endotoxin or an exotoxin. Both identify a faster rate of killing when worms are exposed to live bacteria, and a slower rate when they are exposed to dead bacteria or bacterial metabolites. The results reported in my study showing *lys-1* induction firmly establishes, for the first time, a pointed immune action by the worms against these bacteria, further supporting conclusions by others that these bacteria are actively engaged in infective action against the worm.

Difference in reported kill rate between worms exposed to a single strain of pathogen under different conditions is well documented in other examples and is so called “fast-killing” or “slow-killing” (Alegado et al. 2003). In other examples, a pathogen will exhibit widely variant kill rates under varying media conditions, and this is due to the richness of the medium: richer medium leads to faster killing and poorer medium leads to slower killing. It is thought to be due to the expression of virulence factors, such as toxins, that are easier for the pathogen to express when it is well nourished. In the case of *Burkholderia* species, there have been no tests exploring bacterial growth condition dependent kill rates, however a slow killing and fast killing effect was used to demonstrate the existence of a toxin.

There is a single paper that reports that *Burkholderia* pathogenesis is due, in part, to the action of an endotoxin (O'Quinn et al. 2001). However, other reports strongly

suggest the existence of an exotoxin in these pathogenic species. For example, Gan et al. (2002) report data that strongly suggest that *C. elegans* is killed by some sort of external metabolite of several *Burkholderia* pathogens, including *B. thailandensis*. In addition, there is a well-documented 31 kilodalton exotoxin in *B. pseudomallei* that is likely also present in *B. thailandensis* (Ismail et al. 1987). There are proteases and tyrosine phosphatases secreted by *B. pseudomallei* that are associated with virulence (Lim et al. 2004). And, there is a report of a 10 kilodalton exotoxin that is directly correlated with pathogenesis of *B. pseudomallei* (Haase et al. 1997). Based on available evidence, there is little doubt that *B. thailandensis* is engaged overtly in exotoxicity. Having shown a clear immune response to *B. thailandensis* in my experiments, I decided to test several genes of known and putative immune function against secreted products of *B. thailandensis* to see if toxins were having a direct impact on the *C. elegans* immune system.

I tested the expression of six genes in worms exposed to conditioned rich medium (see materials and methods). Of these*, lys-1, lys-7, lys-8, nlp-29,*and *abf-1* showed no reproducible change in expression. However, *abf-2* showed pointed and reproducible downregulation, suggesting a possible strategy of immune avoidance by *B. thailandensis. ABF-2* is reported to have potent antimicrobial activity against several Gram negative bacteria (Froy 2005) and is believed to be expressed strongly and constitutively (based on GFP reporters) in the pharyngeal lumen of *C. elegans* (Kato et al. 2002). It could, therefore, be the case that *Burkholderia* are misregulating this by an as-of-yet unidentified mechanism as a way to infect the worm through its mouth. In addition, this

downregulation is clear evidence that the worms are being acted on by some excreted product of this bacterium, corroborating an earlier report by Gan et al. (2002).

In my studies, the expression of *lys-7* was used as evidence of DAF-2 pathway activation, as this gene is one of the known downstream targets of this pathway (Ewbank 2006). Since none of my results show any kind of reproducible pattern of change in the expression of this gene, there is, therefore, no evidence of this pathway's involvement in a response by *C. elegans* to the secreted products of *B. thailandensis*.

Similarly, *lys-8* is a known downstream target of the DBL-1 signaling pathway (Ewbank 2006) and was used in my analysis to provide evidence of this pathway's activation in response to *B. thailandensis.* As with *lys-7*, there is no evidence in my results of this pathway's activation in the worm in response to secreted products of *B. thailandensis*.

Nlp-29 is a known downstream target of TIR signaling, and was used in my experiments as an indicator of potential signaling by this pathway. As with both *lys-7* and *lys-8* there is no clear pattern of upregulation of this gene in response to the secreted products of *B. thailandensis*. Taken together, the result that *lys-7*, *lys-8*, and *nlp-29* do not respond to *B. thailandensis* conditioned medium suggests that three of the major pathways involved in *C. elegans* immune signaling are not involved in the worms response to products, toxins or otherwise, that are secreted by *B. thailandensis.*

My results are, with respect to *abf-2*, consistent with those reported for the *abf-3* gene (Alper et al. 2007). The authors do not discuss this in any great detail, but there is a statistically significant down regulation of *abf-3* in response to *S. marcescens* (strain

IGX2) that they report. Based on my results using conditioned media, there is no evidence that the three pathways that I tested for are activated by *B. thailandensis* exotoxin. This suggests that *abf-2* has a mechanism of regulation independent of these established innate immune pathways. This is in agreement with Alper et al. (2007) who grouped the *abf* genes into a category that is not influenced by any immune signaling pathway.

The fact that *lys-1* was not upregulated in the face of conditioned medium (Figure 5 and Table 5) and was upregulated in response to live *Burkholderia* (Figures 13 and Tables 12) further corroborates the notion that its induction is an immune response to an active pathogenesis, and not a more passive type response, for example, to toxic stress. The fact that this enzyme is upregulated in response to infection by Gram negative bacteria (e.g. *S. marcescens* and *B. thailandensis*) is also of potential interest, as its action is generally most pronounced against Gram positive bacteria (Masschalck and Michiels 2003). It may very well be that pathogens are, in general, able to cause the worm immune system to mount inappropriate responses, and this, in turn, allows the pathogen to infect. More work would be required to demonstrate this conclusively.

The melt curves for reactions run with *nlp-29* and *abf-1* primers (Figures 8 and 9) show multiple products as indicated by two or more peaks. In the case of *nlp-29*, there is only one reported protein sequence (WormBase 2008). It is possible that the multiple PCR products observed in my reactions are the result of splice variants that have not been reported, though there is no solid evidence to back this assertion. Perhaps a more likely explanation is non-specific priming to one or more of the 41 reported paralogs to this

gene in this worm. In the case of *abf-1,* the explanation is likely the same except that there are only 7 reported paralogs to *abf-1*.

The standard curve reactions with a near perfect logarithmic concentration to amplification cycle relationship (calculated empirically) of ~3.3 cycles per 10-fold difference in template copy number (Figure 2, Table 2). The theoretical value of this relationship is $N=N_0E^c$, were N_0 is the number of template molecules at the beginning of the cycle, N is the number of template molecules at the end of the cycle, C, and E is the efficiency of the reaction. The efficiency, theoretically, is between 1 (zero efficiency) and 2 (100% efficiency)(Marino 2003). Based on my data, the dynamic range of the iCycler Real-Time PCR detection system is approximately between 61 ng/mL and 550 fg/mL for the pGEM vector. This is in reasonable agreement with other published results (Bustin 2000, Yang et al. 2007, Ahmad 2007). It is important to note that the range observed is usually reported as total copy number or total copy number per volume, not as a mass. And, the range obtained is influenced by the specific template, in addition to the other PCR parameters. For pGEM, the dynamic range is from approximately 835 total template molecules to $1.84x10^9$ total template molecules. This range is in reasonable agreement with other published results.

Bioinformatics of Defensin-like proteins

Because I observed a marked downregulation of *abf-2* expression in response to *B. thailandensis,* I began searching the human genome for sequences related, in property, to ABF sequences. As discussed in the introduction, ABF polypeptides are defensin-like,

and as shown in Table 13, there is a great deal of property similarity within this class of molecule. Of the examples shown in Table 13, most are less than 100 amino acids in length and all are less than 200. In addition, all are cysteine rich, most have basic predicted isoelectric points, all but 2 have transmembrane segments near the amino-terminus, all but one have hydropathy plots that include a strongly hydrophobic amino-terminal sequence stretch followed by a more central hydrophilic stretch (Figure 16), and most have dozens of significant protein blast hits. All of these properties are expected based on the reported characteristics of Defensins (Froy 2005, Zhang and Kato 2003) and antimicrobial peptides (Jenssen et al. 2006). The strong similarity in the output from these *in silico* tools when they are applied to defensin-like peptide sequences suggests that it may be possible to identify novel, as-of-yet unidentified antimicrobials using these output parameters. It seems reasonable to suggest, due to the fact that numerous CSαβ-type polypeptides contain these features, that putative polypeptides showing these features may be either CSαβ-type or, if not specifically CSαβ-type, antimicrobial non-the-less.

Of the 130 short Gnomon-predicted sequences that I screened, not one had all of these characteristics, and the vast majority had none of these characteristics (Figures 17 and 18, and Table 14). However, several of the sequences had multiple matching characteristics to those of defensin-like peptides, and some were missing only the cysteine richness. These sequences missing cysteine richness, however, still have the potential to form at least one disulfide bridge, which is a common feature of antimicrobial peptides, CSαβ-type and not (Jenssen et al. 2006).

It is potentially of great importance that many studies discussing homology, convergent evolution, and properties of defensin-like peptides emphasize the cysteine residues as defining and important structural characteristics of these polypeptides (Jenssen et al. 2006, Froy 2005, Zhang and Kato 2003, Pillai et al. 2003, Kato et al. 2002). My results suggest that there may be multiple proteins encoded by the human genome that have multiple defensin-like properties *except* that they lack cysteine richness (Figures 18 through 21, and Table 14). The most stark of the examples I discovered are the Gnomon-predicted sequences hmm132143 and hmm120686. Both of these have predicted isoelectric points in the basic range, predicted transmembrane sequences, defensin-like hydropathy profiles, short amino acid length, a secretory signal in the amino-terminal region (data not shown), significant sequence identity to other known human defensins (Figures 19 through 21), and at least a dozen significant hits in a protein blast search. In addition, one of these sequences (hmm132143) has a predicted cleavage site in the appropriate location (Bendtsen et al. 2004) and is designated as a reference sequence in the NCBI database, though no known function is listed.

It may be the case that there are many polypeptides, that are, in fact, antimicrobial but have been overlooked in searches for defensins and other CSαβ-type peptides due to lack of numerous cysteine residues. To determine whether this is truly the case, further experimentation is required to elucidate what, if any, function these putative peptides have. I suggest the following: 1) synthesize the putative sequences identified here and test them *in vitro* for antimicrobial properties, and 2) if they are antimicrobial, then screen

multiple genomes for peptides sequences that fit all the *in silico* properties of the sequences discussed here and begin screening those as well.

CONCLUSION

Over 200 years after the creation of the science of immunology, infective disease is still one of the leading causes of death on earth. In more recent times, the study of immunology has begun to focus more strongly than ever on highly conserved innate mechanisms, some of which possibly originate in evolution prior to the appearance of eukaryotic cells. Studies of innate immune mechanisms present in invertebrate organisms have had profound impact on our understanding of the human immune system and the nature of human disease. The nematode worm *Caenorhabditis elegans* is an effective model invertebrate for the study of host pathogen interactions in human disease. The bacterium *Burkholderia thailandensis* (a direct and nearly identical relative to the causative agent of melioidosis) kills *C. elegans* via a fast-killing infection that involves both an active pathogenesis and the action of at least one secreted toxin. The worm, in turn, responds with a clear yet ineffective immune response. At least one secreted product of *B. thailandensis* causes a downregulation of ABF-2, a defensin-like peptide molecule likely to have microbicidal activity against this bacterium, and this, in turn, may represent part of a broader pathogenic strategy of this bacterium to misregulate important immune genes. Sequence mining in the human genome revealed putative peptide sequences that have multiple property similarity, and high sequence identity, to known human defensins. These putative defensin-like peptides may have been overlooked in previous studies due to lack of cysteine richness.

LITERATURE CITED

Ahmad AI 2007. BOXTO as a real-time thermal cycling reporter dye. Journal of Biosciences 32: 229-239.

Akira S, Uematsu S & Takeuchi O 2006. Pathogen recognition and innate immunity. Cell 124: 783-801.

Alegado RA, Campbell MC, Chen WC, Slutz SS & Tan MW 2003. Characterization of mediators of microbial virulence and innate immunity using the Caenorhabditis elegans host-pathogen model. Cellular Microbiology 5: 435-444.

Alper S, McBride SJ, Lackford B, Freedman JH & Schwartz DA 2006. Specificity and complexity of the Caenorhabditis elegans innate immune response. Molecular and Cellular Biology 27: 5544-5553.

Ambion, Applied Biosystems, 850 Lincoln Centre Dr. Foster City, CA 94404 USA.

Ausubel FM, Brent R, Kingston RE, Moore DD, Seidman JG, Smith JA & Struhl K (Editors) 1995. Short protocols in molecular biology: third edition. John Wiley and Sons, Inc. New York.

Bendtsen JD, Nielsen H, von Heijne G & Brunak S 2004. Improved prediction of signal peptides: SignalP 3.0. Journal of Molecular Biology 340: 783-95.

Beutler B 2004. Innate immunity: an overview. Molecular Immunology 40: 845-859.

Biology workbench 2003. San Diego Supercomputer Center, MC 0505, 10100 Hopkins Drive, La Jolla, CA 92093-0505 http://workbench.sdsc.edu/

Borish LC & Steinke JW 2003. Cytokines and chemokines. The Journal of Allergy and Clinical Immunology 111: S460-S474.

Brett PJ, DeShazer D & Woods DE 1998. *Burkholderia thailandensis* sp. nov., a *Burkholderia pseudomallei*-like species. International Journal of Systematic Bacteriology 48: 317-320.

Bustin SA. 2000. Absolute quantification of mRNA using real-time reverse transcription polymerase chain reaction assays. Journal of Molecular Endocrinology 25: 169-93.

Cheng AC & Currie BJ 2005. Melioidosis: epidemiology, pathophysiology, and management. Clinical Microbiology Reviews 18: 383-416. Couillault C, Pujol N, Reboul J, Sabatier L, Guichou JF, Kohara Y & Ewbank JJ 2004. TLR-independent control of innate immunity in *Caenorhabditis elegans* by the TIR domain adaptor protein TIR-1, an ortholog of human SARM. Nature Immunology 5: 488-494.

DeVeale B, Brummel T & Seroude L 2004. Immunity and aging: the enemy within? Aging Cell 3: 195-208.

Ewbank JJ 2006. Personal communication. Centre d'Immunologie de Marseille-Luminy INSERM U631, CNRS UMR 6102, 163 Avenue de Luminy, Case 90613288 Marseille Cedex 9, France.

Ewbank JJ 2002. Tackling both sides of the host-pathogen equation with *Caenorhabditis elegans*. Microbes and Infection 4: 247-256.

Froy O 2005. Convergent evolution of invertebrate defensins and nematode antibacterial factors. Trends in Microbiology 13: 314-319.

Gan YH, Chua KL, Chua HH, Liu B, Hii CS, Chong HL & Tan P 2002. Characterization of *Burkholderia pseudomallei* infection and identification of novel virulence factors using a *Caenorhabditis elegans* host system. Molecular Microbiology 44: 1185-1197.

García-Lara J, Needham AJ & Foster SJ 2005. Invertebrates as animal models for *Staphylococcus aureus* pathogenesis: a window into host-pathogen interaction. FEMS Immunology and Medical Microbiology 43: 311-323.

Garsin DA, Sifri CD, Mylonakis E, Qin X, Singh KV, Murray BE, Calderwood SB & Ausubel FM. 2001. A simple model host for identifying Gram-positive virulence factors. Proceedings of the National Academy of Sciences of the United States of America 98: 10892-10897.

Gerttula S, Jin YS & Anderson KV 1988. Zygotic expression and activity of the *Drosophila* Toll gene, a gene required maternally for embryonic dorsal-ventral pattern formation. Genetics 119: 123-33.

Gibson UE, Heid CA & Williams PM 1996. A novel method for real time quantitative RT-PCR. Genome Research 6: 995-1001.

Glass MB, Gee JE, Steigerwalt AG, Cavuoti D, Barton T, Hardy RD, Godoy D, Spratt BG, Clark TA & Wilkins PP 2006. Journal of clinical microbiology. 44: 4601-4604.

Gröne A 2002. Keratinocytes and Cytokines. Veterinary Immunology and Immunopathology 88: 1-12.

Gravato-Nobre MJ & Hodgkin J 2005. *Caenorhabditis elegans* as a model for innate immunity to pathogens. Cellular Microbiology 7: 741-751.

Haase A, Janzen J, Barrett S & Currie B 1997. Toxin production by *Burkholderia pseudomallei* strains and correlation with severity of melioidosis. Journal of Medical Microbiology 46: 557-563.

Hejazi A & FR Falkiner 1997. *Serratia marcescens*. Journal of Medical Microbiology. 46: 903-912

Invitrogen Corporation 1600 Faraday Avenue PO Box 6482 Carlsbad, California 92008

Ismail G, Noor Embi M, Omar O, Allen JC, Smith CJ. 1987. A competitive immunosorbent assay for detection of *Pseudomonas pseudomallei* exotoxin. Journal of Medical Microbiology. 23(4):353-357.

Janeway C, Travers P, Walport M & Shlomchik M 2005. Immunobiology: the immune system in health and disease. Sixth edition. New York: Garland Science Publishing P. 37-100.

Jenner E., M.D., F.R.S. 1801. An inquiry into the causes and effects of the Variolae Vaccinae, a disease discovered in some of the western counties of England, particularly Gloucestershire, and known by the name of the cow-pox, Third edition. London: printed for the author by D. N. Shury.

Jenssen H, Hamill P & Hancock RE 2006. Peptide antimicrobial agents. Clinical Microbiology Reviews 19: 491-511.

Kato Y, Aizawa T, Hoshino H, Kawano K, Nitta K & Zhang H 2002. *Abf-1* and *abf-2*, ASABF-type antimicrobial peptide genes in *Caenorhabditis elegans*. Biochemical Journal 361: 221-230.

Kim DH & Ausubel FM 2005. Evolutionary Perspectives on innate immunity from the study of *Caenorhabditis elegans*. Current Opinion in Immunology 17: 4-10.

Köllisch G, Kalali BN, Voelcker V, Wallich R, Behrendt H, Ring J, Bauer S, Jakob T, Mempel M & Ollert M 2005. Various members of the Toll-like receptor family contribute to the innate immune response of human epidermal keratinocytes. Immunology 114: 531-541.

Kurz CL & Ewbank JJ 2003. *Caenorhabditis elegans*: an emerging genetic model for the study of innate immunity. Nature Reviews Genetics 4: 380-390.

Kyte J & Doolittle RF 1982. A simple method for displaying the hydropathic character of a protein. Journal of Molecular Biology 157: 105-32.

Leippe M 1999. Antimicrobial and cytolytic polypeptides of amoeboid protozoa effecter molecules of primitive phagocytes. Developmental and Comparative Immunology 23: 267-279.

Lemaitre B, Nicolas E, Michaut L, Reichhart JM & Hoffmann JA 1996. The dorsoventral regulatory gene cassette spätzle/Toll/cactus controls the potent antifungal response in *Drosophila* adults. Cell 86: 973-83.

Lim KP, Li H & Nathan S 2004. Expression and purification of a recombinant scFv towards the exotoxin of the pathogen, *Burkholderia pseudomallei*. Journal of Microbiology 42: 126-132.

Mallo GV, Kurz CL, Couillault C, Pujol N, Granjeaud S, Kohara Y & Ewbank JJ 2002. Inducible antibacterial defense system in *C. elegans.* Current Biology 12: 1209-1214.

Marino JH, Cook P & Miller KS 2003. Accurate and statistically verified quantification of relative mRNA abundances using SYBR Green I and real-time RT-PCR. Journal of Immunological Methods 283: 291-306.

Masschalck B & Michiels CW 2003. Antimicrobial properties of lysozyme in relation to foodborne vegetative bacteria. Critical Reviews in Microbiology 29: 191-214.

Mazumdar PMH 2003. History of immunology. In: Paul WE, editor. Fundamental immunology: fifth edition. New York: Lippincott Williams & Wilkins. P 23-46.

Medzhitov R 2003. The innate immune system. In: Paul WE, editor. Fundamental immunology: fifth fdition. New York: Lippincott Williams & Wilkins. P. 497-517.

Millet AC & Ewbank JJ 2004. Immunity in *Caenorhabditis elegans*. Current Opinion In Immunology 16: 4-9.

Mylonakis E. & Aballay A 2005. Worms and flies as genetically tractable animal models to study host-pathogen interactions. Infectious Immunology 73: 3833-3841.

National Center For Biological Information 2007. http://www.ncbi.nlm.nih.gov/blast/Blast.cgi

National Center For Biological Information 2003. http://www.ncbi.nlm.nih.gov/genome/guide/gnomon.html

O'Quinn AL, Wiegand EM & Jeddeloh JA 2001. *Burkholderia pseudomallei* kills the nematode *Caenorhabditis elegans* using an endotoxin-mediated paralysis. Cellular Microbiology: 381-393.

Paul WE 2003. The immune system: an introduction. In: Paul WE, editor. Fundamental immunology: fifth edition. New York: Lippincott Williams & Wilkins. P. 1-22.

Persson B & Argos P 1994. Prediction of transmembrane segments in proteins utilizing multiple sequence alignments. Journal of Molecular Biology 237: 182-92.

Peterson SV, Thiel S & Jensenius JC 2001. The mannan-binding lectin pathway of complement activation: biology and disease association. Molecular Immunology 38: 133-149.

Pillai A, Ueno S, Zhang H & Kato Y 2003. Induction of ASABF (*Ascaris suum* antibacterial factor)-type antimicrobial peptides by bacterial injection: novel members of ASABF in the nematode *Ascaris suum*. The Biochemical Journal. 371: 663-668.

Pradel E & Ewbank JJ 2004. Genetic models in pathogenesis. Annual Review of Genetics 38: 347-363.

Rock FL, Hardiman G, Timans JC, Kastelein RA & Bazan JF 1998. A family of human receptors structurally related to *Drosophila* Toll. Proceedings of the National Academy Science USA 95: 588-593.

Santana MA & Esquivel-Guadarrama F 2006. Cell biology of T-cell activation and differentiation. International Reviews of Cytology 250: 217-274.

Schröder JM & Harder J 2006. Antimicrobial skin peptides and proteins. Cellular and Molecular Life Sciences 63: 469-486.

Schulenburg H, Kurz CL & Ewbank JJ 2004. Evolution of the innate immune system: the worm perspective. Immunological Reviews 198: 36-58.

Sifri CD, Begun J & Ausubel FM 2005. The worm has turned – microbial virulence modeled in *Caenorhabditis elegans*. Trends in Microbiology 13: 119-127.

Sims PJ & Wiedmer T 1995. Induction of cellular procoagulant activity by the membrane attack complex of complement. Seminars in Cell Biology 6: 275-282.

Sjöholm AG, Jönsson G, Braconier JH, Sturfelt G Truedsson L. 2006. Complement Deficiency and Disease: An Update. Molecular Immunology. 43: 78-85.

Thompson JD, Higgins DG, Gibson TJ. 1994. CLUSTAL W: improving the sensitivity of progressive multiple sequence alignment through sequence weighting, position-specific gap penalties and weight matrix choice. Nucleic Acids Research 22: 4673-4680.

Tlaskalová-Hogenová H, Tucková L, Lodinová-Zádniková R, Stepánková R, Cukrowska B, Funda DP, Striz I, Kozáková H, Trebichavský I, Sokol D, Reháková Z, Sinkora J, Fundová P, Horáková D, Jelínková L & Sánchez D 2002. Mucosal immunity: its role in defense and allergy. International Archives of allergy and immunology 128: 77-89

Toldo L 1995. http://www.embl-heidelberg.de/cgi/pi-wrapper.pl

Turner MW & Hamvas RM 2000. Mannose-binding lectin: structure, function, genetics and disease associations. Reviews in Immunogenetics 2: 305-322.

WormBase 2007. http://www.wormbase.org/

Woo PC, Woo GK, Lau SK, Wong SS & Yuen K 2002. Single gene target bacterial identification. groEL gene sequencing for discriminating clinical isolates of *Burkholderia pseudomallei* and *Burkholderia thailandensis*. Diagnostic Microbiology and Infectious Disease 44: 143-149.

Yang ZZ, Habib M, Shuai JB & Fang WH 2007. Detection of PCV2 DNA by SYBR Green I-based quantitative PCR. Journal of Zhejiang University. Science. B 8: 162-169.

Yu Y, Kim HS, Chua HH, Lin CH, Sim SH, Lin D, Derr A, Engels R, DeShazer D, Birren B, Nierman WC & Tan P 2006. Genomic patterns of pathogen evolution revealed by comparison of *Burkholderia pseudomallei*, the causative agent of melioidosis, to avirulent *Burkholderia thailandensis*. BMC Microbiology 6: 46

Zhang H & Kato Y 2003. Common structural properties specifically found in the CSalphabeta-type antimicrobial peptides in nematodes and mollusks: evidence for the same evolutionary origin? Developmental and Comparative Immunology 27: 499-503.